THE INFLUENCE OF ENERGETIC MESOSCALE
EDDIES ON THE OCEAN THERMAL STRUCTURE

Willine Elizabeth Christensen

NAVAL POSTGRADUATE SCHOOL
Monterey, California

THESIS

THE INFLUENCE OF ENERGETIC MESOSCALE

EDDIES ON THE OCEAN THERMAL STRUCTURE

by

Willine Elizabeth Christensen

March 1976

Thesis Advisor: R. L. Haney

T173119

REPORT DOCUMENTATION PAGE		READ INSTRUCTIONS BEFORE COMPLETING FORM
1. REPORT NUMBER	2. GOVT ACCESSION NO.	3. RECIPIENT'S CATALOG NUMBER
4. TITLE (and Subtitle) The Influence of Energetic Mesoscale Eddies on the Ocean Thermal Structure		5. TYPE OF REPORT & PERIOD COVERED Master's Thesis March 1976
		6. PERFORMING ORG. REPORT NUMBER
7. AUTHOR(s) Willine Elizabeth Christensen		8. CONTRACT OR GRANT NUMBER(s)
9. PERFORMING ORGANIZATION NAME AND ADDRESS Naval Postgraduate School Monterey, CA 93940		10. PROGRAM ELEMENT, PROJECT, TASK AREA & WORK UNIT NUMBERS
11. CONTROLLING OFFICE NAME AND ADDRESS Naval Postgraduate School Monterey, CA 93940		12. REPORT DATE March 1976
		13. NUMBER OF PAGES 53
14. MONITORING AGENCY NAME & ADDRESS(if different from Controlling Office) Naval Postgraduate School Monterey, CA 93940		15. SECURITY CLASS. (of this report) Unclassified
		15a. DECLASSIFICATION/DOWNGRADING SCHEDULE

16. DISTRIBUTION STATEMENT (of this Report)

Approved for public release; distribution unlimited.

17. DISTRIBUTION STATEMENT (of the abstract entered in Block 20, if different from Report)

18. SUPPLEMENTARY NOTES

19. KEY WORDS (Continue on reverse side if necessary and identify by block number)

20. ABSTRACT (Continue on reverse side if necessary and identify by block number)

The influence of internal heating by mesoscale eddies on the oceanic temperature structure is tested by including a vertical heat transport term, $\overline{w'T'}$, in the ocean thermal budget equation. The value for this term was determined from a theoretical study by Gill, Green and Simmons (1974). In the past studies of the thermocline problem, the heat transport term has been neglected. Analytical and numerical test cases were run solving the heat equation with and without the mesoscale eddy heat transport term for baroclinic

DD FORM 1473 EDITION OF 1 NOV 65 IS OBSOLETE
1 JAN 73
(Page 1)   S/N 0102-014-6601 |

and barotropic conditions in the ocean. Whenever heating by mesoscale eddies was included in the heat equation, excessive cooling occurred in the upper 1000 m of the ocean. The results of the test cases indicate that the eddies do have a distinct influence on the ocean's thermal structure and need to be included in solutions to the heat equation for the ocean.

The Influence of Energetic Mesoscale

Eddies on the Ocean Thermal Structure

by

Willine Elizabeth Christensen
Lieutenant, United States Navy
B.A., Whitworth College, 1967

Submitted in partial fulfillment of the
requirements for the degree of

MASTER OF SCIENCE IN METEOROLOGY

4

ABSTRACT

The influence of internal heating by mesoscale eddies on the oceanic temperature structure is tested by including a vertical heat transport term, $\overline{w'T'}$, in the ocean thermal budget equation. The value for this term was determined from a theoretical study by Gill, Green and Simmons (1974). In the past studies of the thermocline problem, the heat transport term has been neglected. Analytical and numerical test cases were run solving the heat equation with and without the mesoscale eddy heat transport term for baroclinic and barotropic conditions in the ocean. Whenever heating by mesoscale eddies was included in the heat equation, excessive cooling occurred in the upper 1000 m of the ocean. The results of the test cases indicate that the eddies do have a distinct influence on the ocean's thermal structure and need to be included in solutions to the heat equation for the ocean.

TABLE OF CONTENTS

LIST OF FIGURES

ACKNOWLEDGEMENTS

The author wishes to express her thanks to Dr. Robert L. Haney for his guidance given throughout the preparation of this thesis.

Special appreciation is given to the night-shift personnel of the W. R. Church Computer Center and to a number of understanding friends who have been patient with me during the writing of this thesis.

I. INTRODUCTION

In recent years scientists have found that highly energetic, rotating water masses exist in the ocean below the mixed layer. Eddies, as these masses have been called, appear to be similar to the high and low pressure systems in the atmosphere. Their origin and the extent of their influence on the temperature structure of the ocean is not fully known. Meteorologists as well as oceanographers are showing an increasing interest in these eddies as a means of obtaining a better understanding of the parameters of air-sea interactions.

In 1970 a group of scientists began preparations that would lead to documentation of the existence of eddies. The Mid-Ocean Dynamics Experiment (MODE) was a multi-national experiment conducted in the area between Bermuda and Florida. Through extensive measurements of currents, temperature, salinity and pressure the scientists discovered the existence of two types of eddies; deep water eddies and highly energetic eddies in the upper 1500 meters of the ocean.

It is the purpose of this paper to study the possible influence of the upper-layer eddies on the thermal structure of the ocean following the methods used in previous studies of the oceanic thermocline. These thermocline theories are all based on the assumptions of geostrophic and hydrostatic balance, incompressibility, neglect of salinity and some form of the steady state first law of thermodynamics which in most general form is

$$u \frac{\partial T}{\partial x} + v \frac{\partial T}{\partial y} + w \frac{\partial T}{\partial z} = \kappa \frac{\partial^2 T}{\partial z^2} \qquad (1)$$

Table I gives a list of symbols and constants used in this study. The general balance expressed by (1) is a balance between horizontal and vertical advection and vertical diffusion of heat. Stommel and Webster (1962) have considered the simple barotropic case which balances vertical advection and vertical diffusion. Robinson and Stommel (1958) ignore the effects of east-west temperature advection (term one of (1)) while Welander (1971) considers a balance of all the terms in equation (1). In each of the above studies, the effect of mesoscale heating was ignored.

The plan of this study is to consider the simplest model in which the effect of heating by mesoscale eddies given by the term, $\frac{\partial}{\partial z}(\overline{w'T'})$, can be added to (1). If the energy source for the eddies is available potential energy, then $\overline{w'T'}$ and its vertical derivative will not be zero. Since the eddies have been verified by the MODE data, it therefore becomes important to examine the effect that this term may have on solutions to the thermocline problem. For this study, the correlation term, $\frac{\partial}{\partial z}(\overline{w'T'})$ was specified according to theoretical results of Gill, Green and Simmons (1974) for a baroclinically unstable eddy of wavelength 322 km.

Since the solution to the heat equation used for this study depends on the amplitude of $\overline{w'T'}$, its profile with depth and on the wind forced Ekman vertical velocity, cases were run to test each of these factors. Analytical and numerical solutions are found for the cases in which the Ekman wind and then the mesoscale heating are set equal to zero respectively. A numerical solution is found when both the wind forcing and the internal heating are included. In all cases horizontal temperature

10

TABLE I. Symbols and Values of Constants

t   time

w   vertical velocity

T   perturbation temperature

R   radius of Earth

ϕ latitude, 36°N

λ longitude

Ω angular speed of Earth's rotation, 2π day^{-1}

α thermal expansion coefficient, 2.0×10^{-4} (°K)$^{-1}$

f   coriolis parameter, $2\Omega \sin \phi$

v   northward velocity component

u   eastward velocity component

κ vertical eddy viscosity and conductivity, .5 cm^2 sec^{-1}

advection is ignored. The results obtained in this study indicate

that the effect of baroclinically unstable eddies on the ocean tempera-

ture profile is significant.

II. EQUATION AND MODEL DEVELOPMENT

A. HEAT EQUATION

The basic heat budget equation for the ocean is

$$\frac{dT}{dt} = Q/\rho c_p \qquad (2)$$

where Q represents the convergence of net incoming and outgoing radiation. It is assumed that radiative exchange takes place in the first few meters of the ocean. The model designed for this study is such that the level of $z = 0$ is at the bottom of the surface Ekman layer. This implies that within the ocean itself

$$\frac{dT}{dt} = 0 \qquad (3)$$

Expanding (3) and writing it in flux form gives

$$\frac{\partial T}{\partial t} + \nabla \cdot (VT) = 0 \qquad (4)$$

Let $V = \bar{V} + V'$ and $T = \bar{T} + T'$ where at this point the primes denote all turbulent motions including the baroclinic mesoscale eddies. A time average sufficient to remove all the turbulent motions (say 120 days) is performed with the result

$$\frac{\partial T}{\partial t} + \bar{V} \cdot \nabla \bar{T} + \nabla \cdot (\overline{V'T'}) = 0 \qquad (5)$$

13

Expanding this into component parts and making the simplifying assumption that advection and heat transfer by turbulence in the north-south and east-west directions can be ignored gives the following equation

$$\frac{\partial \overline{T}}{\partial t} + \overline{w} \frac{\partial \overline{T}}{\partial z} + \frac{\partial}{\partial z} (\overline{w'T'}) = 0 \tag{6}$$

The turbulent vertical transport of heat, $(\overline{w'T'})$, can be thought of as being accomplished by two distinct physical processes. The first is through transport by baroclinic mesoscale eddies represented by the term $(\overline{w'T'})_{mesoscale}$ where the subscript of mesoscale will be assumed for the rest of this paper. The second means of heat transfer is by all other turbulent motions. This transfer is assumed to be adequately represented by vertical diffusion of heat down the mean temperature gradient; $-\kappa \frac{\partial \overline{T}}{\partial z}$. The final equation to be solved is therefore

$$\frac{\partial \overline{T}}{\partial t} + \overline{w} \frac{\partial \overline{T}}{\partial z} + \frac{\partial}{\partial z} (\overline{w'T'} - \kappa \frac{\partial \overline{T}}{\partial z}) = 0 \tag{7}$$

where $\overline{w'T'}$ now represents the heat transport by mesoscale eddies.

B. M EQUATION

This study follows the approach of Welander (1971) who considered the solution to a similar heat equation for the thermocline region, but without the heating due to mesoscale eddies. The steady state, geostrophic, hydrostatic equations in a region away from side boundaries are

$$-fv = -\frac{1}{R\cos\phi} P_\lambda \ , \ fu = -\frac{1}{R} P_\phi \ , \ P_z = g\alpha T$$

$$\frac{1}{R} \cos\phi \ \{u\lambda + (v\cos\phi)_\phi\} + w_z = 0$$

$$\frac{u}{R\cos\phi} T_\lambda + \frac{v}{R} T_\phi + w T_z = \kappa T_{zz}$$

14

where the variable P and T are perturbation pressure and perturbation temperature. Salinity is neglected and the assumptions of a spherical earth, ocean depth H small compared to the radius of the earth and constant density in the horizontal direction are made. Following Needler (1967), Welander derived a non-linear equation for pressure of fourth order and second degree. Noting the difficulty in solving the equation for pressure he defined a new function

$$M(\lambda,\phi,z) = \int_0^z p\,dz + 2\Omega R^2 \sin^2\phi \int_0^\lambda w_0\,d\lambda \qquad (8)$$

which is a first integral of pressure. The function also incorporates a boundary condition since w_0 is the vertical velocity at the bottom of the surface Ekman layer. Welander points out that in general $(u,v) \neq 0$ at the bottom thus implying a barotropic component. The M function provides the following definitions:

$$u = \frac{1}{2\Omega R \sin\phi} M_{\phi z} \qquad\qquad v = \frac{1}{2\Omega R \sin\phi \cos\phi} M_{\lambda z}$$

$$w = \frac{1}{2\Omega R^2 \sin^2\phi} M_\lambda \qquad P = M_z \qquad T = \frac{1}{g\alpha} M_{zz}$$

Substituting these definitions into the heat equation (7) developed for consideration in this thesis, an M equation similar to Welander is obtained

$$\frac{\partial}{\partial t}(M_{zz}) + \frac{1}{2\Omega R^2 \sin^2\phi} M_\lambda M_{zzz} - \kappa M_{zzzz} + g\alpha \frac{\partial}{\partial z}(\overline{w'T'}) = 0 \qquad (9)$$

Letting

$$M_{zz} = \theta \qquad (10)$$

and assuming

$$\kappa \neq \kappa(z)$$

there results

$$\theta_t + \frac{1}{2\Omega R^2 \sin^2 \phi} M_\lambda \theta_z - \kappa \theta_{zz} + g\alpha \frac{\partial}{\partial z}(\overline{w'T'}) = 0 \qquad (11)$$

The first term of (11) is proportional to the local time change of tem-
perature. The second term represents the vertical advection of mean
temperature while the third term is the vertical diffusion of the mean
temperature. The last term is the heating due to mesoscale eddies.
Numerical solutions to equations (10) and (11) for a steady state were
obtained using the initial value approach. Analytic solutions were also
obtained in the simplest cases. Before discussing analytic and numerical
solutions to (10) and (11), a detailed description of the boundary condi-
tions will be given.

C. BOUNDARY CONDITIONS

    The physical model chosen to test the influence of ocean eddies is
shown in Figure 1. The model is tested in a region of the Pacific Ocean
away from any strong boundary currents, along 36°N. The domain was
chosen to be large compared to the size of an eddy and to be sufficiently
small so that the atmospheric forcing could be considered approximately
uniform. A flat bottom was assumed for the two dimensional model. For
initial test cases the boundary conditions were independent of longitude
making this a one-dimensional model (solution independent of x).

    Since equation (9) is of fourth order, four boundary conditions can
be applied to the problem. An advantage of using Welander's M function
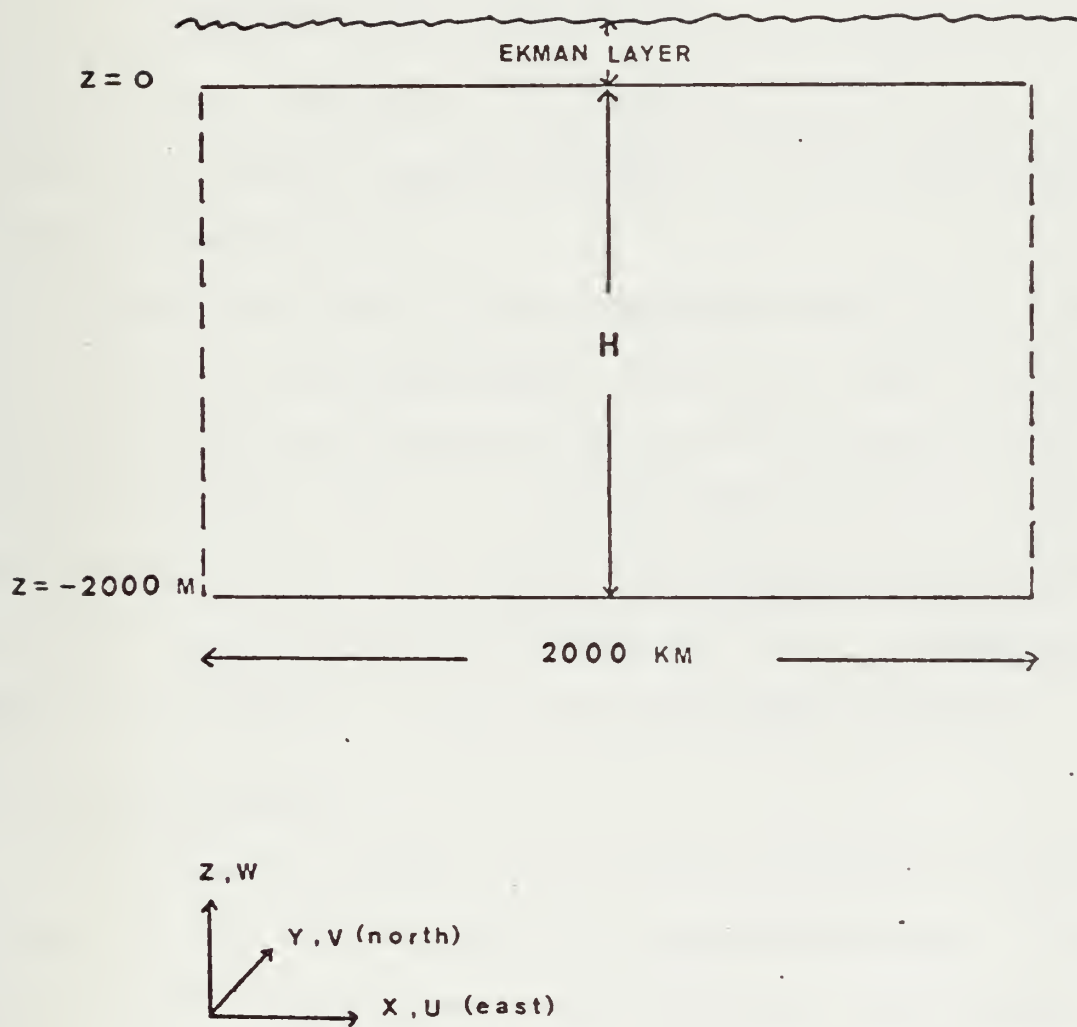
16

Figure 1.   Two dimensional model along 36°N with $\Delta z = 40$m and $\Delta x = 80$m.

is that part of the boundary conditions are incorporated in the function itself. In practice it was convenient to solve (10) and (11) as the system

$$M_{\lambda zz} = \theta_\lambda \qquad (12)$$

$$\frac{\partial \theta}{\partial t} + \frac{1}{2\Omega R^2 \sin^2\phi} M_\lambda \theta_z - \kappa\theta_{zz} + g\alpha \frac{\partial}{\partial z} (\overline{w'T'}) = 0 \qquad (13)$$

These are solved conveniently with boundary conditions on M_λ at the ocean top and bottom in equation (12) and on θ at the ocean top and bottom in equation (13).

The model has a rigid lid with w prescribed at the top and bottom. At z = 0, M_λ at the surface becomes $2\Omega R^2 \sin^2\phi\, w_o$ where w_o is a pre-scribed vertical motion produced by the wind at the bottom of the surface Ekman layer. At z = -H , the boundary condition is w = 0 , which requires $M_\lambda = 0$. The thermal conditions at the top and at the bottom are to prescribe the temperatures T_o and T_{-H} respectively. Thus, at the surface $\theta = g\alpha\, T_o$ and at the bottom, $\theta = g\alpha\, T_{-H}$.

D. EDDY HEAT TRANSFER

In this thesis no attempt has been made to parameterize the eddy transfer of heat, $\overline{w'T'}$, in terms of the dependent variables. No direct measurements of the heat transfer were available so it was necessary to resort to theory to obtain an estimate. In a paper by Gill, Green and Simmons (1974) a theoretically determined rate of conversion of avail-able potential energy to eddy kinetic energy is developed as a function of z in a vertically continuous model. The values of $\overline{w'T'}$ presented by Gill et al are those that would exist if the mesoscale eddies were the

18

result of _in situ_ baroclinic instability. As such, the $\overline{w'T'}$ which is used in this paper is based on a given horizontal and vertical profile of temperature. Figure 2 from Gill et al shows $\overline{w'T'}$ as a function of depth for eddies of four different wavelengths. The amplitudes associated with these profiles are based on the assumption that all of the available potential energy in the mean flow is converted into the eddies. This study can be thought of as a test of this assumption as well as a test of the _in situ_ baroclinic instability theory. Figure 3 shows the mean velocity which determines the temperature profile.

For analytic treatment in this thesis the heat flux due to mesoscale eddies was expressed as an exponential function.

$$\overline{w'T'} = A\ e^{z/D} \tag{14}$$

where A , .0357 °C cm sec^{-1}, is the amplitude and D , 100 m , is the characteristic depth of energy transfer. The profile of $\frac{\partial}{\partial z}(\overline{w'T'})$ is shown in Figure 4. This corresponds in amplitude and profile to that shown in (b) of Figure 2. The large amplitude indicates an extremely strong upward flux of heat in the upper 500 m of the ocean.

Fig. 12. The rate of conversion of available potential energy to eddy energy, shown as a function of depth. The scale is chosen so that the integral with respect to depth (in m) gives B m W m^{-4} s^{-4}. The cases shown are [1] $s = 0$, $k = 0.033$ km^{-1}, [1] $s = 0$, $k = 0.0195$ km^{-1}, [2] $k = 0.0285$ km^{-1}, [3] $k = 0.0275$ km^{-1}.

Figure 2. Profile of the rate of conversion of available potential energy to kinetic energy. From Gill, Green and Simmons (1974).

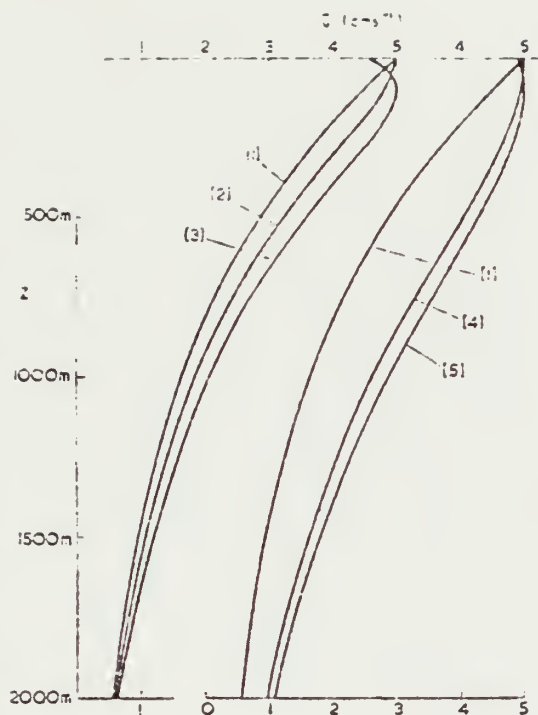Fig. 7. Mean velocity profiles $\bar{U}(z)$ for which a stability analysis has been carried out. For clarity, profiles [4] and [5] have been displaced to the right and profile [1] is drawn twice. Note that the scale of z is limited to less than half the total depth. The mean currents below 2000 m are very small.

Figure 3.   Mean velocity profiles from Gill, Green and Simmons (1974) used to determine temperature profiles.
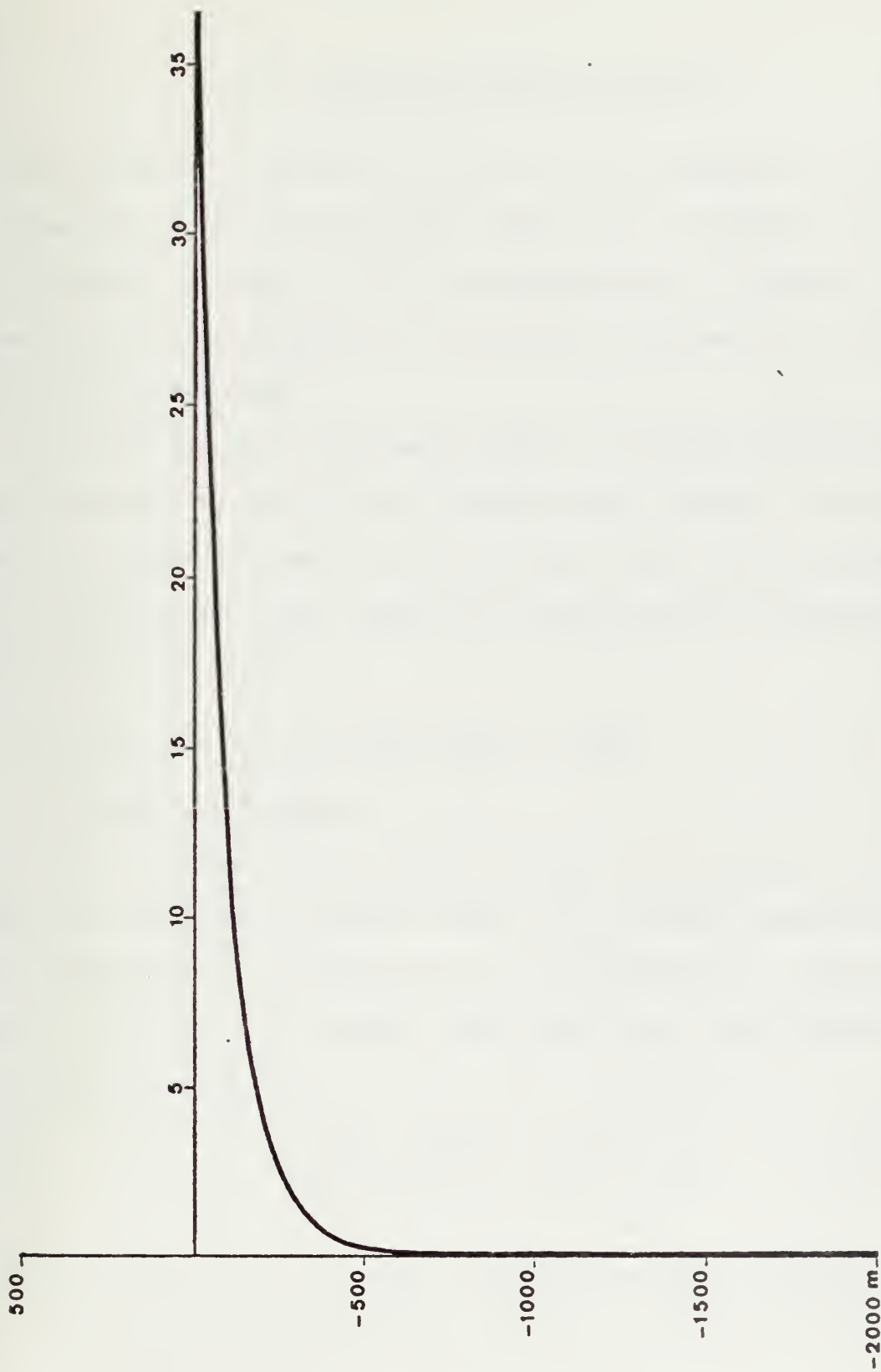
Figure 4. Profile of vertical derivative of $\overline{w'T'}$ showing a large upward flux in the first 500m. Units are °C sec^{-1} x 10^{-7}.

22

III. ANALYTIC AND NUMERICAL RESULTS

The solutions to equations (12) and (13) are dependent on the inter-
nal heating and the surface boundary conditions of temperature and verti-
cal velocity. In order to aid in the interpretation of the more general
numerical solutions, analytical solutions were obtained for a variety of
the simpler cases first.

The first case to be examined was that of no Ekman forcing and the
next case was that of no internal mesoscale eddy heating. The final case
was the most general case which included both Ekman forcing and heating
by mesoscale eddies. Both upward and downward vertical velocities were
tested where applicable.

A. VERTICAL MOTION AT THE SURFACE EQUAL TO ZERO

1. Analytical Solution

In the first case the vertical motion at the bottom of the surface
Ekman layer, w_o, was set equal to zero. If the surface temperature, T_o,
is independent of x, the solution, θ, is independent of x. Therefore by
equation (12), $M_\lambda = 0$ everywhere. The steady state form of equation (13)
thus becomes (using (14))

$$\kappa \frac{\partial^2 T}{\partial z^2} = \frac{\partial}{\partial z}(\overline{w'T'}) = \frac{A}{D} e^{z/D} \tag{15}$$

This is the equation for a local, one-dimensional model without vertical
advection. The analytic solution to (15) was obtained by integrating the

diffusion term twice and applying the boundary conditions of $T(0) = T_o$ and $T(-H) = T_{-H}$.

$$T(z) = T_o + \frac{z}{H} \{(T_o - T_{-H}) - \frac{AD}{K}(1-e^{-H/D})\} - \frac{AD}{K}(1-e^{z/D}) \quad (16)$$

The solution (16) is shown in Figure 5. The temperature is forced to a value of -554°C at approximately 360 m below the surface. The extremely unrealistic nature of this solution indicates that if the open ocean contains mesoscale eddies with the above heating profile, then the thermal balance cannot be maintained by simple downward heat diffusion with $K = .5$ cm^2 sec^{-1}.

2. Numerical Solution

In order to test the numerical model which will be used later for the more general case, a numerical solution to

$$T_t = KT_{zz} - \frac{\partial}{\partial z}(\overline{w'T'}) \quad (17)$$

was obtained. The numerical method is the initial value integration starting from an initial temperature field given by

$$T(z) = T_1 e^{z/d_1} - T_2 e^{z/d_2} \quad (18)$$

The initial profile was defined to meet the stable condition of $\frac{\partial T}{\partial z} \geq 0$. For this to hold the following constants were chosen; $T_1 = 22.5°C$, $T_2 = 2.5°C$, $d_1 = 900$ m and $d_2 = 100$ m. Figure 6 shows this profile.

The general numerical finite difference scheme to solve (17) used a centered differencing in space and time except for the diffusion
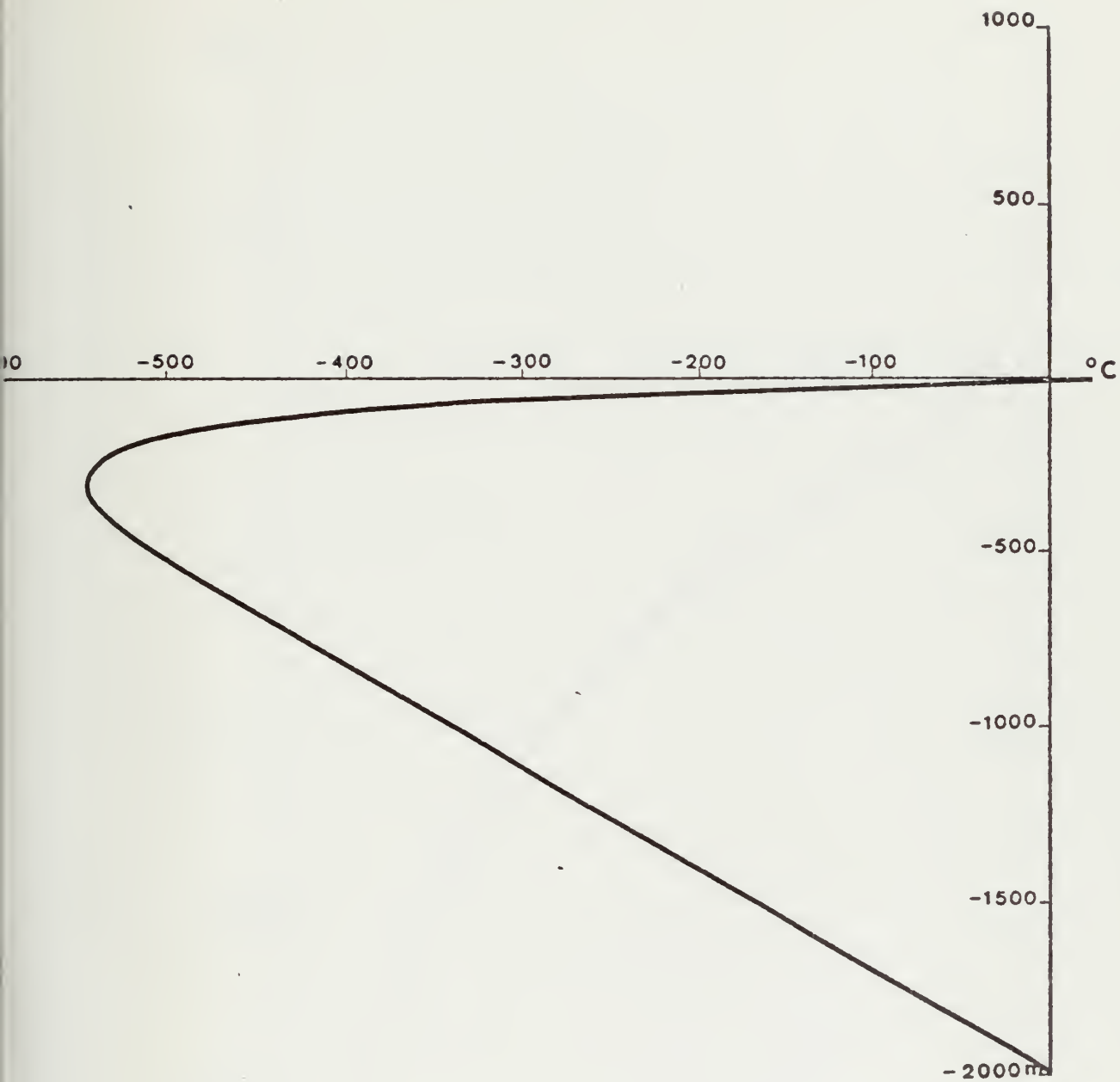
24

Figure 5. Analytic solution to the case in which wind forcing is
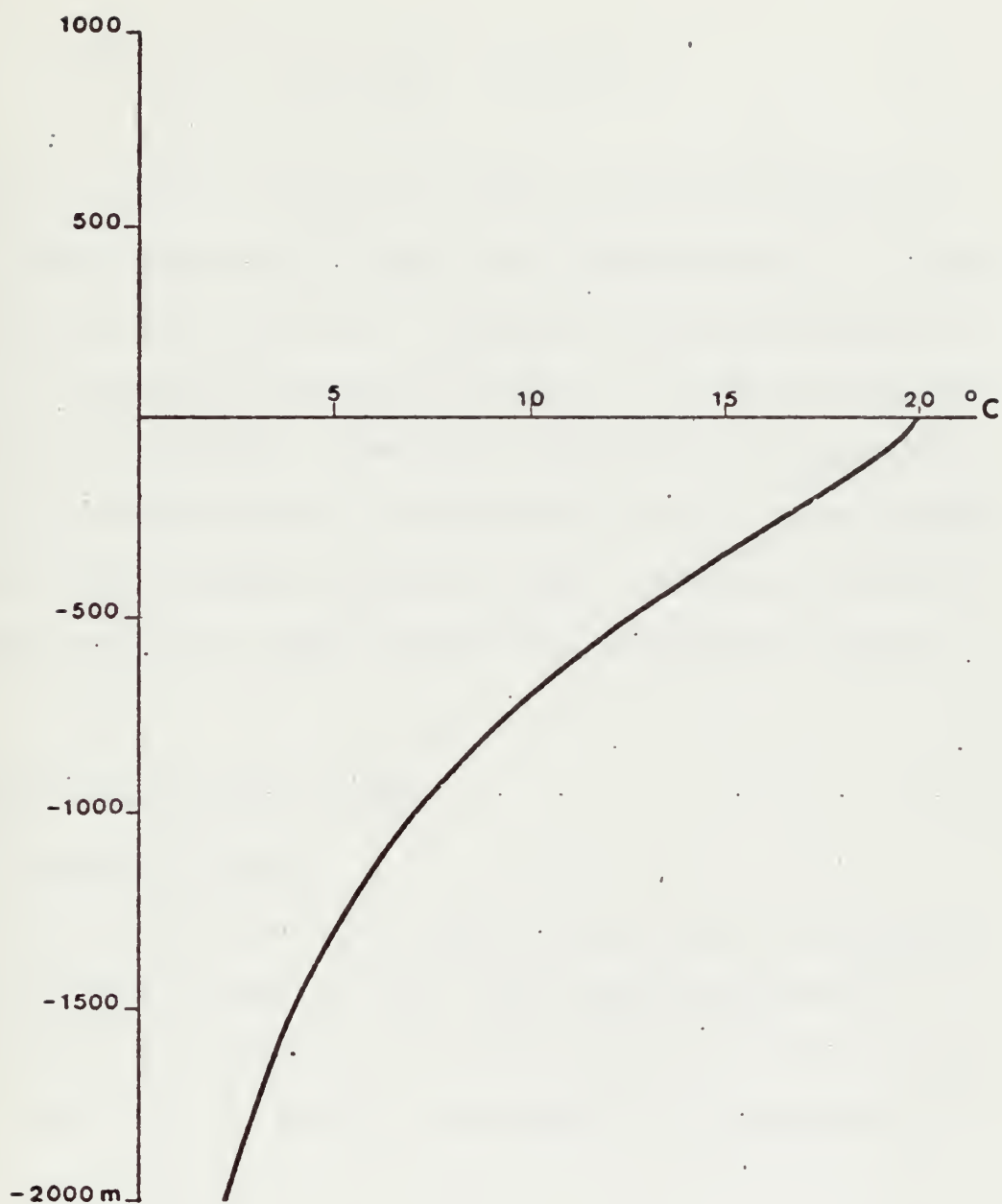equal to zero.

Figure 6. Initial temperature (°C) profile for numerical model.

term which utilized a forward time step. The finite difference analogue is

$$T^{n+1} = T^{n-1} + 2\Delta t(\kappa T^{n-1}_{zz} - g\alpha \frac{\partial}{\partial z}(\overline{w'T'})) \tag{19}$$

where Δt = 10 days, Δz = 40 m, Δx = 80 km. The final solution was reached after integrating for approximately 2000 years and is in agreement with the analytic solution. Intermediate solutions showing the approach to steady state are shown in Figure 7. It can be noted that the forcing term, $\frac{\partial}{\partial z}(\overline{w'T'})$, immediately works to cool the temperature in the top 100 meters and then the diffusion term acts to redistribute the cooler water throughout the entire layer. Solutions to the baroclinic case forced by a thermal gradient are considered in section D below.

B. INTERNAL FORCING EQUAL TO ZERO

   1. Analytical Solution

        In the second case to be tested the heating due to mesoscale eddies, $\overline{w'T'}$, was set equal to zero. This required that there be a balance between heat diffusion and vertical temperature advection for steady state. From (12) and (13) the equations to be solved were

$$\frac{2\Omega R^2 \sin^2\phi}{g\alpha} w_{zz} = T_\lambda \tag{20}$$

$$\kappa \frac{\partial^2 T}{\partial z^2} = w \frac{\partial T}{\partial z} \tag{21}$$

If the surface conditions, T_o and w_o, are independent of x, equation (2) reduces to w_{zz} = 0 with solution

$$w = w_o(1 + \frac{Z}{H}) \tag{22}$$
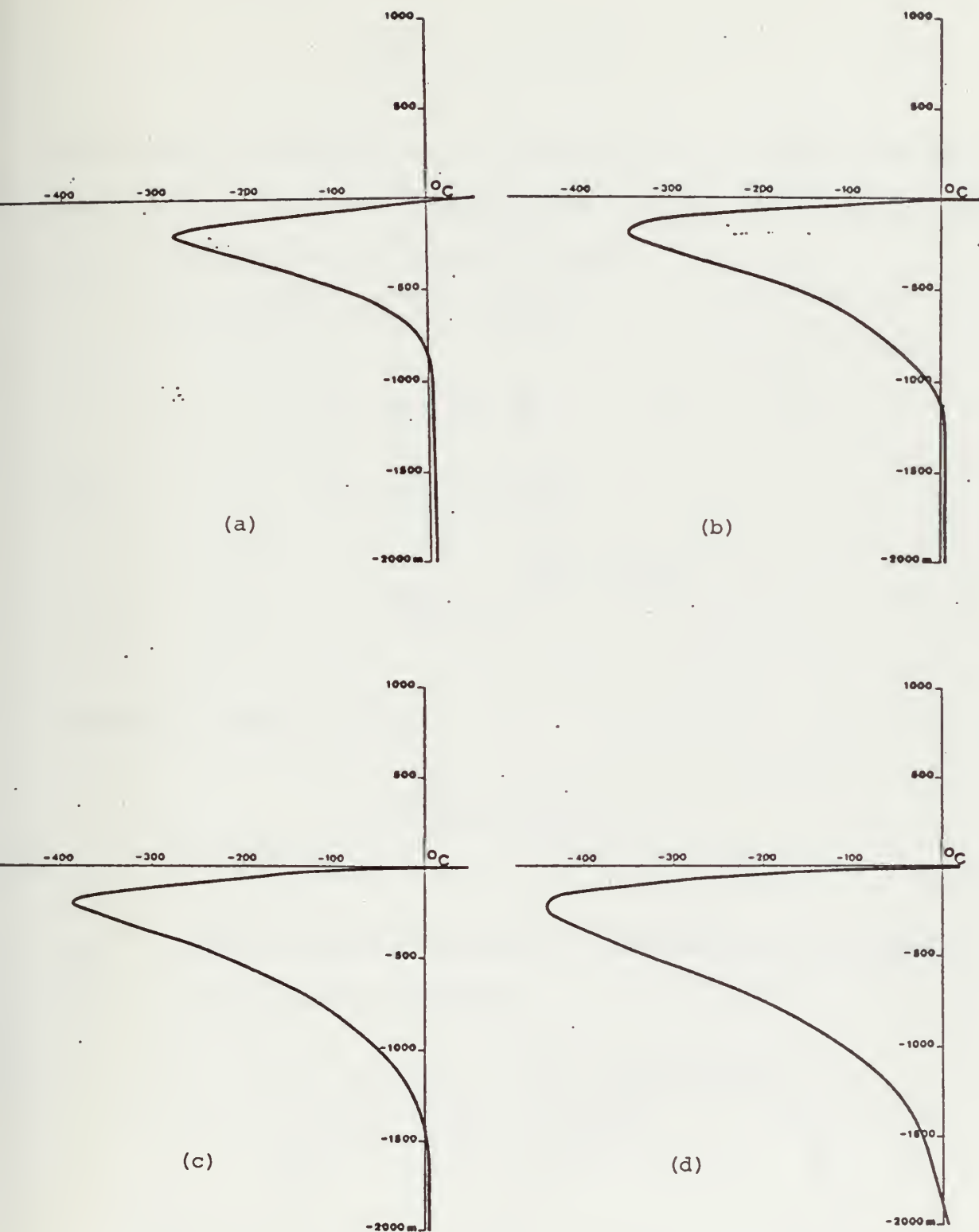
Figure 7.   Intermediate numerical solution to case in which
            wind forcing equal to zero. a) 28 years   b) 55
            years   c) 82 years   d) 165 years.

The equation to solve is thus

$$\kappa \frac{\partial^2 T}{\partial z^2} = w_o (1 + \frac{Z}{H}) \frac{\partial T}{\partial z} \qquad (23)$$

with boundary conditions $T(0) = T_o$ and $T(-H) = T_{-H}$. This is the local, one-dimensional equation with Ekman forced vertical motion of 10 cm day^{-1} but no heating due to the mesoscale eddies.

Let $y = \frac{\partial T}{\partial z}$, then (23) becomes

$$\frac{y'}{y} = \frac{w_o}{\kappa} (1 + \frac{Z}{H})$$

Thus,

$$\ell n y = \frac{w_o}{\kappa} (Z + \frac{z^2}{2H}) + c_1 ,$$

or

$$y = \frac{\partial T}{\partial z} = c_2 e^{\frac{w_o}{\kappa}(Z + z^2/2H)}$$

Integrating from $-H$ to Z;

$$T(Z) - T_{-H} = c_2 \int_{-H}^{Z} e^{\frac{w_o}{\kappa}(\eta + \eta^2/2H)} d\eta$$

where η is the variable of integration. Evaluating c_2 by requiring $T(0) = T_o$, gives the final solution

$$T(Z) = T_{-H} + \left[\frac{T_o - T_{-H}}{\int_{-H}^{o} e^{\frac{w_o}{\kappa}(\eta + \eta^2/2H)} d\eta} \right] \left[\int_{-H}^{Z} e^{\frac{w_o}{\kappa}(\eta + \eta^2/2H)} d\eta \right] \qquad (24)$$

The solution is not in closed form but is given by an integral which must be calculated numerically. The results of equation (24)

being obtained by numerical integration using the trapezoidal rule are shown in Figure 8. Notice that the stratification is confined to the upper 500 m.

Stommel and Webster (1962) have analyzed a similar case in which vertical heat diffusion and heat advection are balanced. Their solution in the barotropic case shows upward vertical velocity a linear function of depth, as in (22), but the temperature is isothermal. The similarity transform used to solve their coupled equations does not allow vertical temperature stratification in the barotropic case. Figure 9 shows the case from Stommel and Webster (1962) in which the w and T lines denoted by 0° (implying a zero horizontal temperature gradient) are for the barotropic case. The stratified temperature profile obtained in this study is allowed because equations (12) and (13) are solved without any restrictions imposed by a similarity transformation.

2. Numerical Solutions

In order to check the numerical model, the same case of no heating by mesoscale eddies was solved numerically. By assuming that the local temperature change with time, $\frac{\partial T}{\partial t}$, is not equal to zero, an initial value time integration was run on the computer. The conditions are identical with those leading to equation (23) so the equation to integrate was

$$\frac{\partial T}{\partial t} = \kappa \frac{\partial^2 T}{\partial z^2} - w_o (1 + \frac{Z}{H}) \frac{\partial T}{\partial z} \tag{25}$$

The finite difference analogue to this was

$$T^{n+1} = T^{n-1} + 2\Delta t (\kappa T_{zz}^{n-1} - w_o (1 + \frac{Z}{H}) T_z^{n}) \tag{26}$$

30
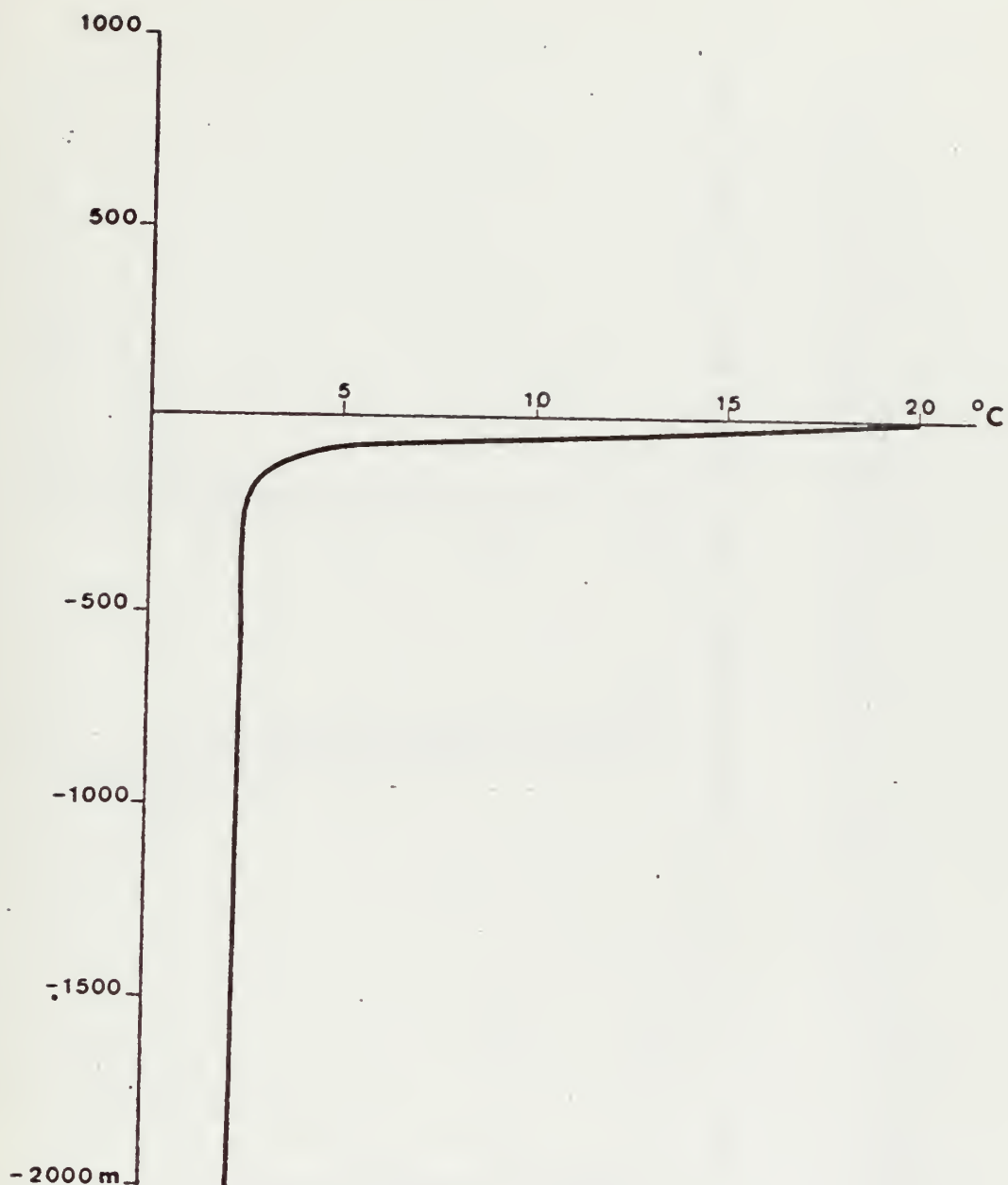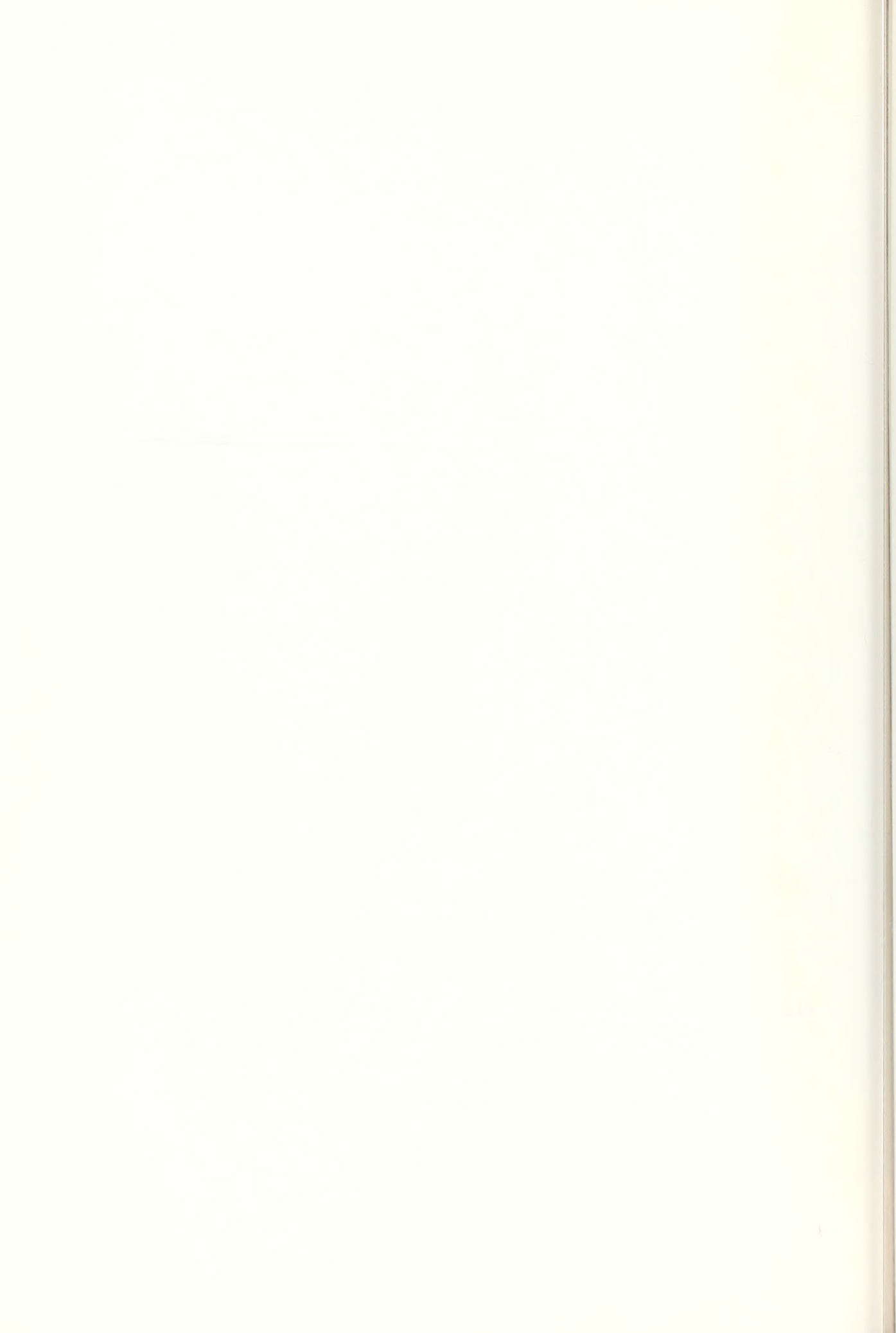
Figure 8. Analytic solution to the case in which heating by meso-
scale eddies is equal to zero with $w_o = 10$ cm day^{-1}.
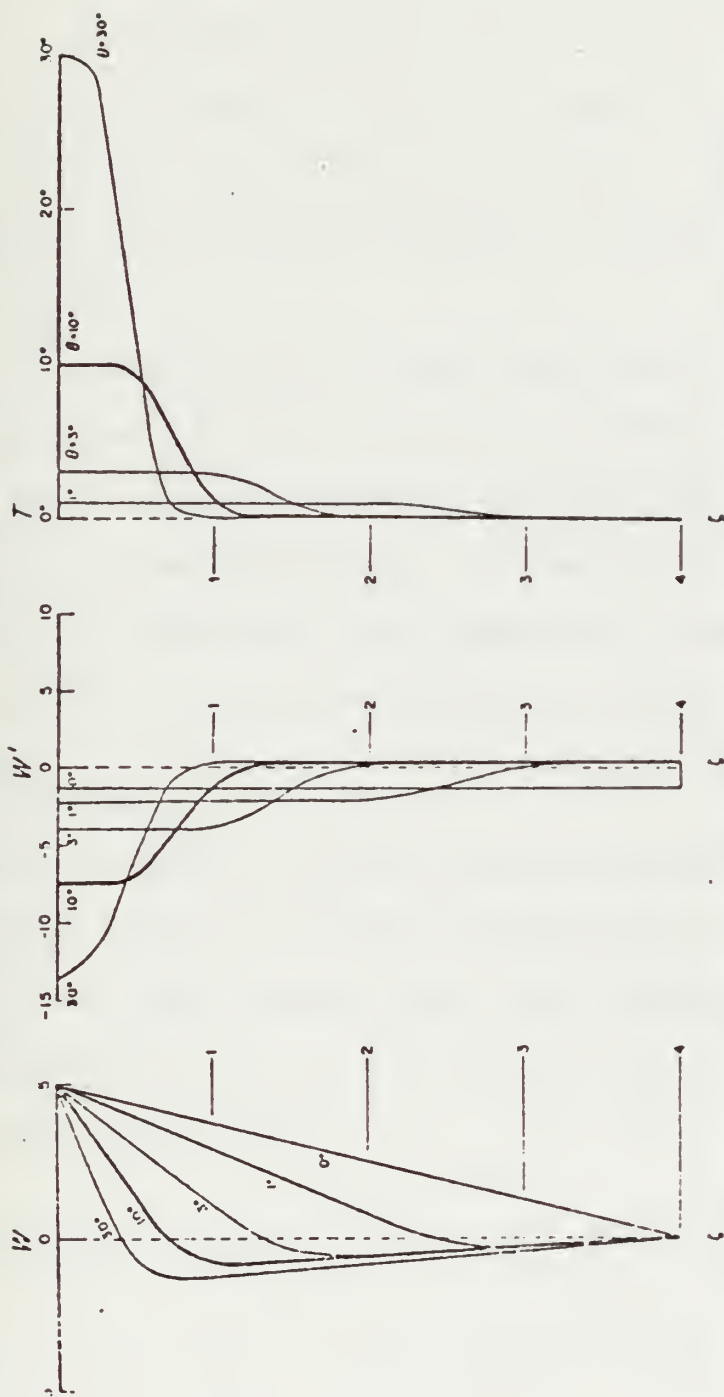
Figure 3. The distribution of W, W', and T, with transformed depth ζ, plotted for various choices of the imposed surface temperature $\vartheta(0)$.

Figure 9. Note the 0° lines (no temperature gradient) which represent the barotropic solution to the balance between $w(\partial T/\partial z)$ and $\kappa(\partial^2 T/\partial z^2)$. From Stommel and Webster (1962).

32

The model was run with a time step of ten days for 1000 years. A steady state was reached after 500 years for the case when $w_o > 0$ (upward motion). The numerical solution agrees with the analytically obtained solution shown in Figure 8. Since the numerically and analytically obtained solutions agree in these simple cases, it is reasonable to trust the accuracy of the numerical solution in the more general cases considered below.

A numerical solution to the case with no internal heating was run with downward vertical velocity of the same magnitude as used before; -10 cm day^{-1}. Figure 10 shows an isothermal condition to great depth with a strong, deep thermocline. It appears that the vertical temperature advection term works in the same sense as the vertical diffusion. Such a profile is clearly not observed in the real ocean.

C. GENERAL CASE

When both physical effects of heating by mesoscale eddies and wind forcing are included recall that the equations to solve are (12) and (13). In the case in which T_o and w_o are independent of x, the solution is independent of x, and so w is given by (22). Equation (13) becomes, with substitution of (22),

$$\frac{\partial \theta}{\partial t} + w_o (1 + \frac{Z}{H}) \; \theta_z - \kappa \theta_{zz} + g\alpha \frac{\partial}{\partial z} \; (\overline{w'T'}) = 0 \qquad (27)$$

The steady state version of this equation is similar to (23) with the addition of the non-homogeneous term and an analytic solution is possible. Due to the complexity of the anticipated solution to equation (27) an analytic solution incorporating all three terms was not obtained.
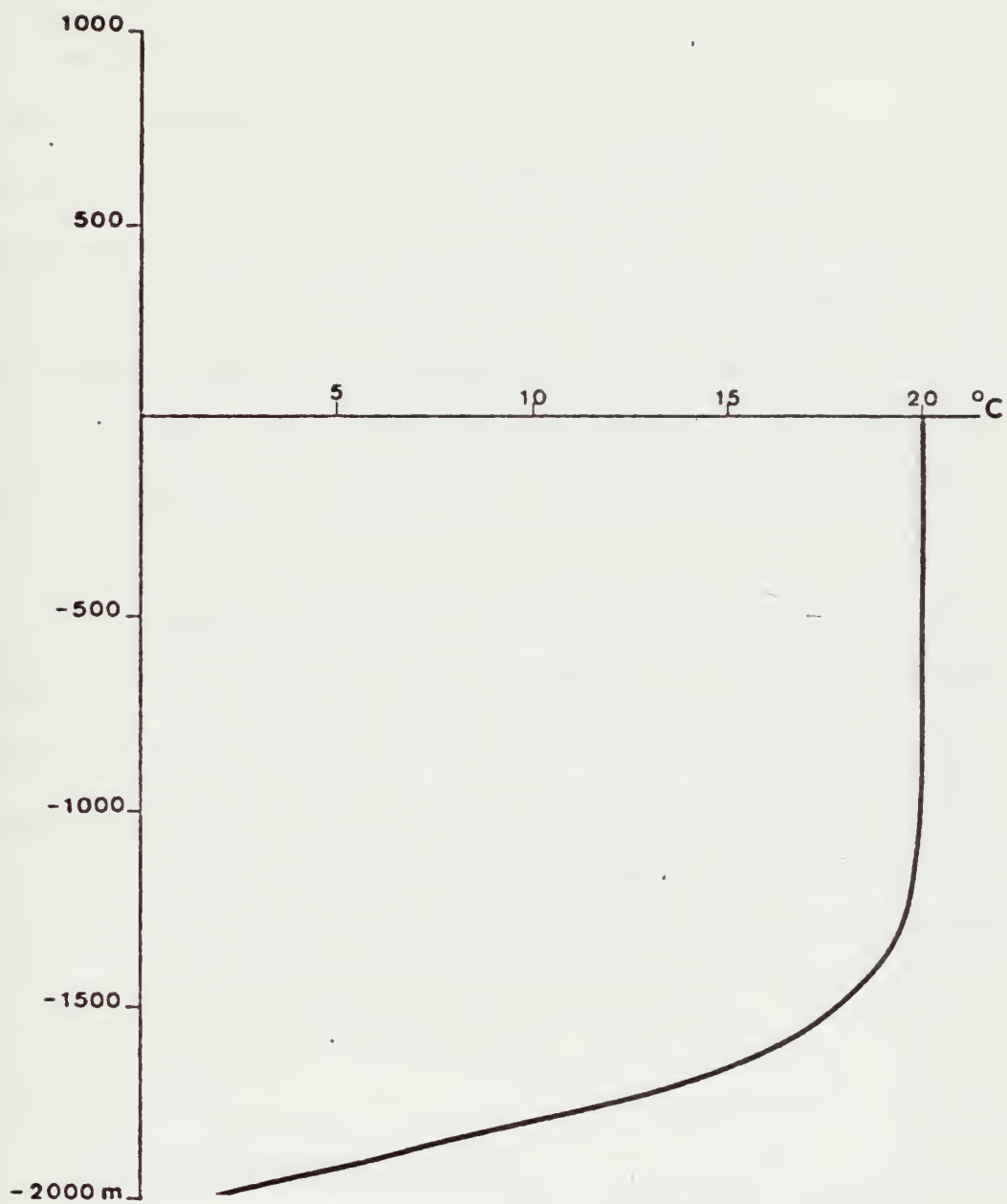
33

Figure 10. Numerical solution to the case in which heating by meso-scale eddies is equal to zero with $w_o = -10$ cm day^{-1}.

Only the initial value numerical method of solution was considered.
Using a time step of ten days steady state solutions, shown in Figures
11 and 12, were reached in approximately 500 years for the cases of
$w_o > 0$ and $w_o < 0$ respectively.

When w_o is upward (Figure 11) the initial temperature change due to
the forcing function is similar to the case when $w_o = 0$ (Figures 5 and
7). The first 250 m are cooled rapidly but then the influence of the
vertical advection slows the cooling which is then confined to the upper
region. The profile is more realistic than that given in Figure 5 for
the case $w = 0$; however the temperature is still an unrealistic $-174\,°C$
at 200 m.

When w_o is downward, the result is seen in Figure 12. Again cooling
takes place quite rapidly due to the influence of the mesoscale eddies.
The downward vertical velocity works with the vertical diffusion so the
deeper waters also experience cooling. It has been shown that none of
the local solutions which contain heating by mesoscale eddies are realis-
tic. Further conclusions will be reached after examining the baroclinic
cases below.

D. BAROCLINIC CASES

    1. Internal Heating Equal to Zero

        The final series of test cases were designed to determine the in-
fluence of heating by mesoscale eddies in a baroclinic ocean. This test-
ing was accomplished by comparing the results obtained with and without
the mesoscale eddy heat transfer term, $\frac{\partial}{\partial z}(\overline{w'T'})$. The initial value
approach to the solution was used with a temperature field having a five
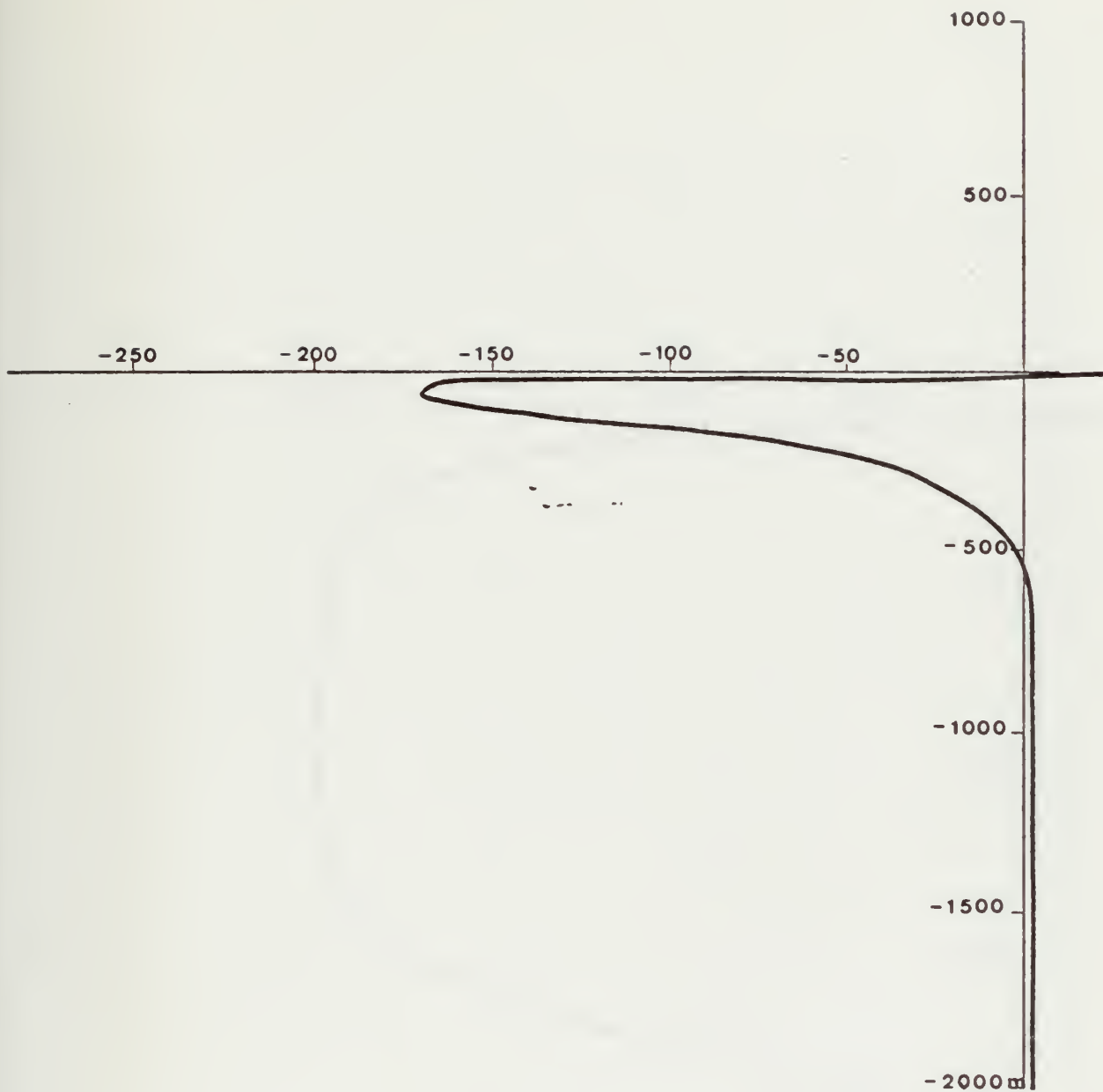degree surface gradient.

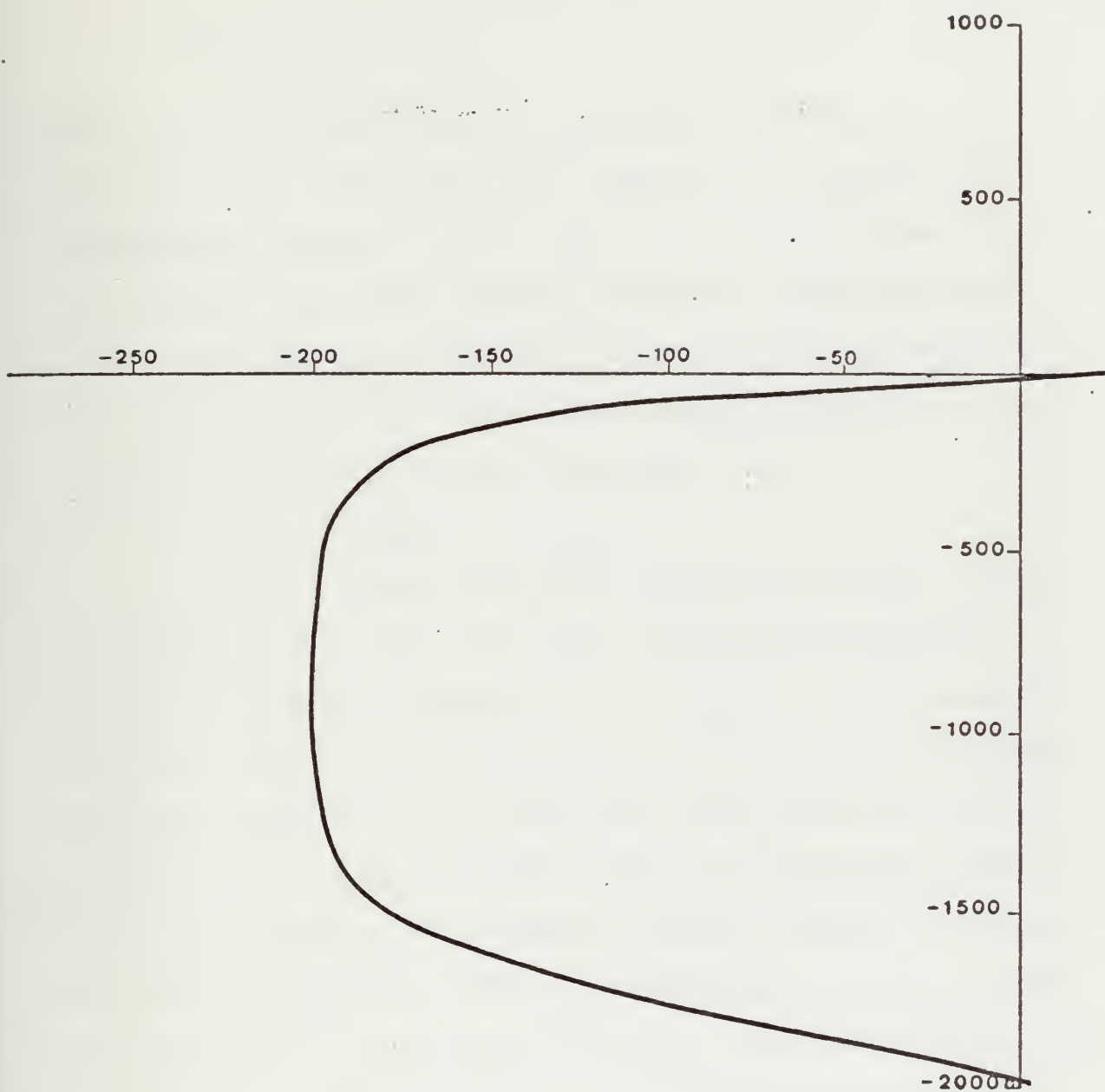Figure 11. Numerical solution to the general case with w_o = +10 cm day^{-1}.

Figure 12. Numerical solution to the general case with $w_o = -10$ cm day^{-1}.

The equation,

$$T(x,z) = (T_1 \pm 5.(x/L))e^{z/d_1} + T_2^{z/d_2} \qquad (28)$$

where L is the east-west extent of the model (2000 km), was used to generate an initial field with either a positive or a negative east-west gradient. The values of $T(x,0)$ and $T(x,-H)$ obtained from (28) constituted the fixed thermal boundary conditions. With the addition of an east-west temperature gradient, the internal vertical motion is now a function of depth and temperature. Because equation (13) is now non-linear, M_λ must be calculated at each time step.

a. Positive Temperature Gradient

Figure 13 shows the initial temperature field with a positive gradient; warmer water to the east. The numerical solution to equations (12) and (13) is shown in Figure 14 for the case when the surface Ekman forcing is greater than zero, $w_o = 10$ cm day^{-1}. An unrealistically deep isothermal layer is depicted. This is also the case for w_o less than zero. A strong interior downward vertical motion, shown in Figure 15, is created by the temperature gradient in both of the above cases. This sinking motion works with the diffusion to cause a packing of the isotherms near the bottom of the ocean. With no other forces acting to counter the double influence of the downward heat advection and diffusion, the resolution of the model is insufficient to handle the strong gradients that finally develop.

b. Negative Temperature Gradient

The initial field with a five degree negative east-west gradient at the surface is shown in Figure 16. When the model was run
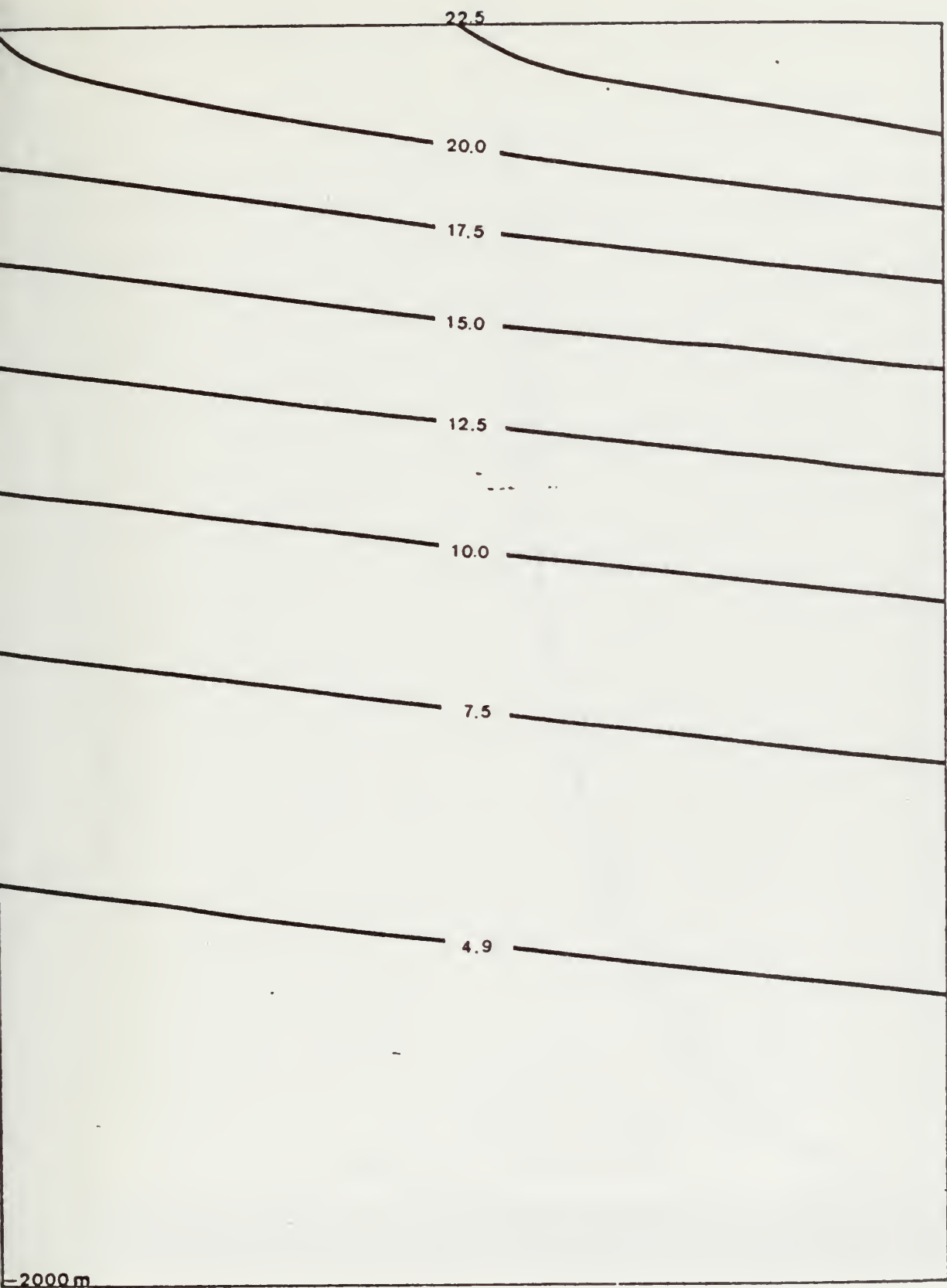
38

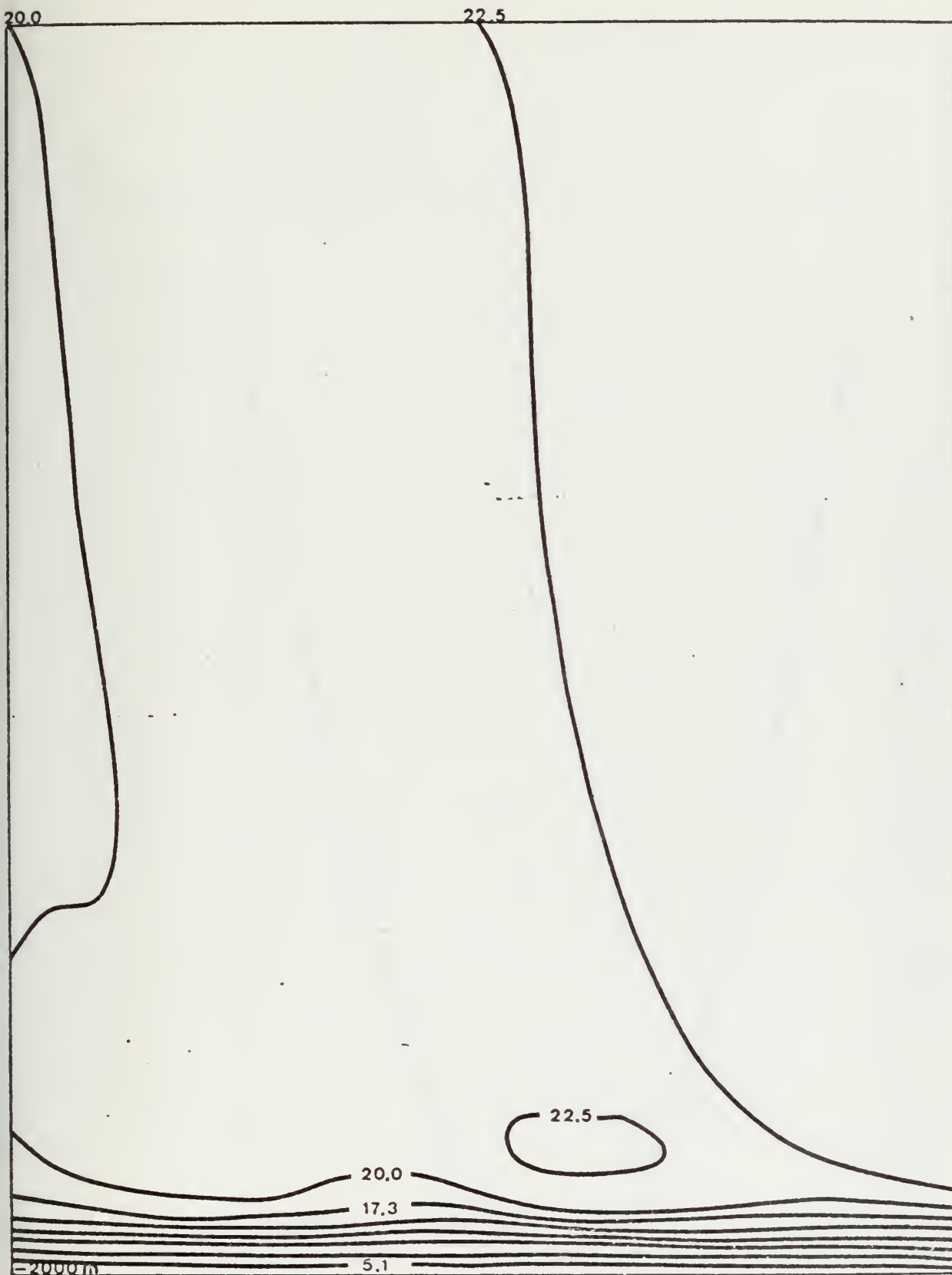Figure 13. Initial temperature field with a 5°C positive gradient in the east-west direction.

Figure 14.   Numerical solution for $(\partial T/\partial x)_o > 0$ and $w_o = 10$ cm day^{-1}, $(\partial/\partial z)\overline{(w'T')} = 0$.   Temperature is in °C.
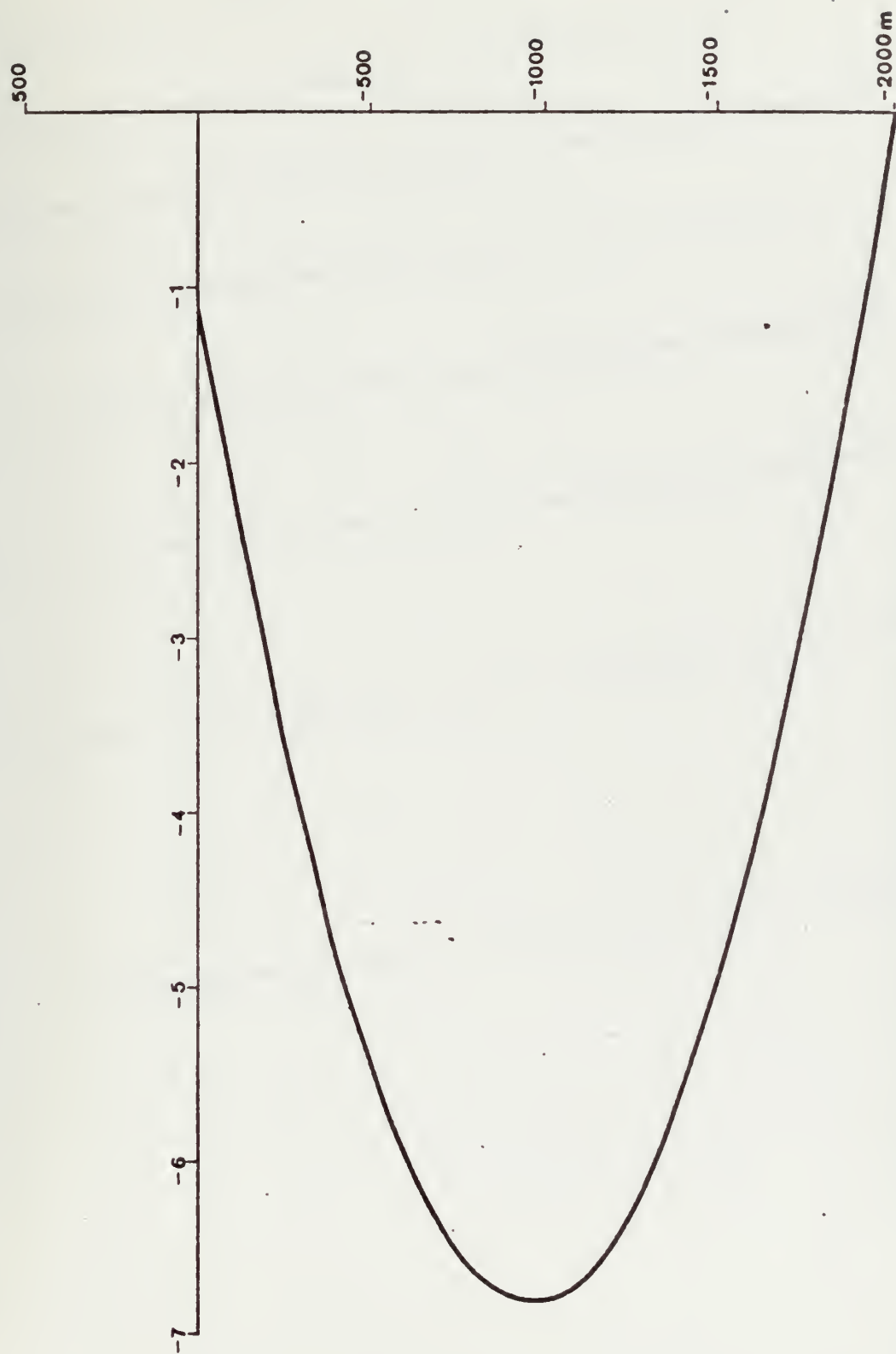
Figure 15. Numerically calculated internal vertical motion for $(\partial T/\partial x)_o > 0$ and $w_o = 10$ cm day^{-1}. w is in cm sec^{-1} x 10^{-4}.
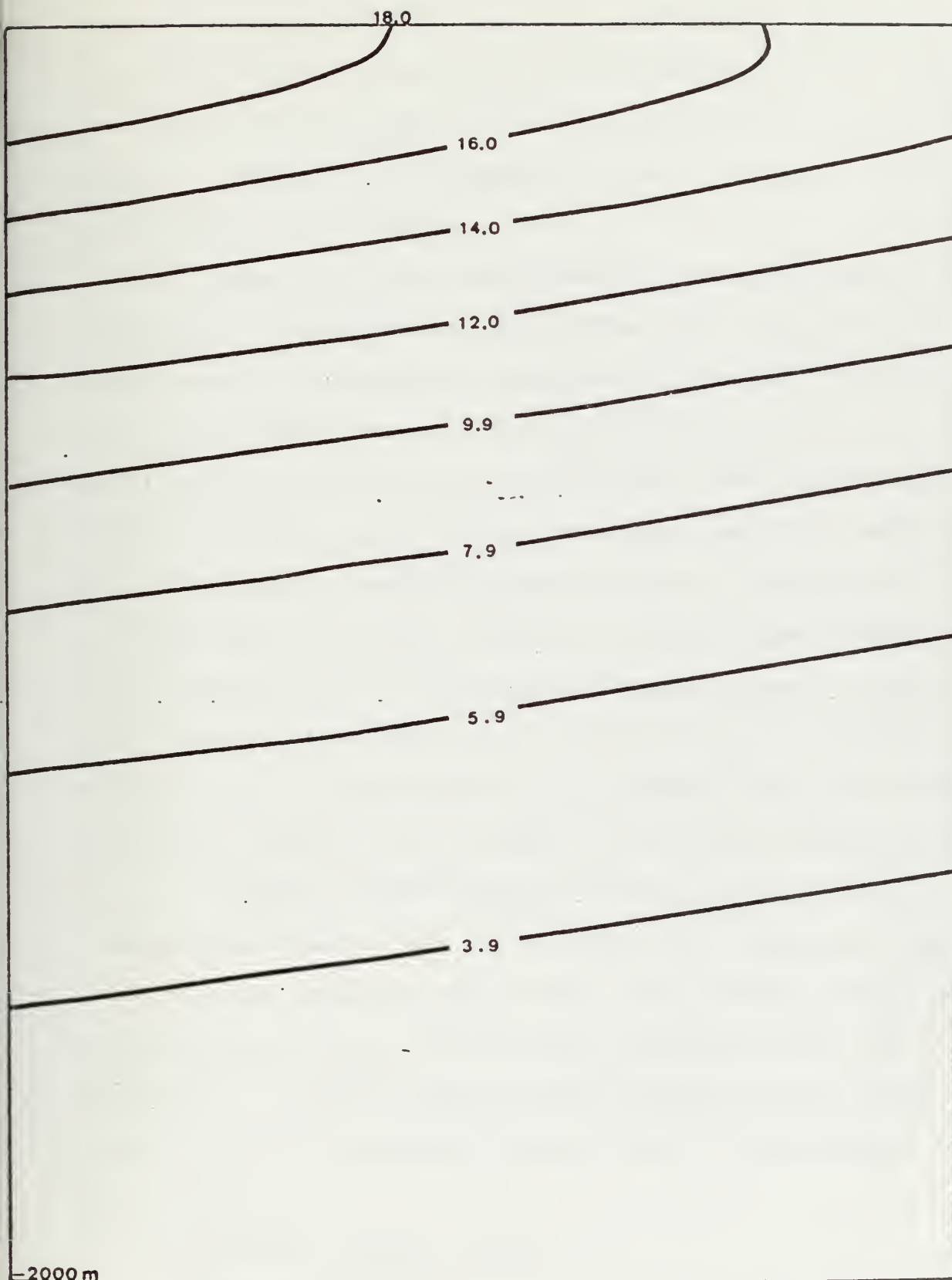
Figure 16.   Initial temperature field with a 5°C negative gradient
in the east-west direction.

with cyclonic wind conditions generating an Ekman layer upward motion

of $w_o = 10$ cm day^{-1}, the resulting interior vertical motion is strongly

positive throughout the model (Figure 17). The resulting vertical ad-

vection is stronger than the downward diffusion and causes a packing of

the isotherms near the surface.

When anticyclonic wind conditions, generating downward ver-

tical motion at the base of the surface Ekman layer, are applied the

interior vertical motion becomes positive only below 250 m. Its maxi-

mum value is smaller than in the previous case in which w_o was positive.

Figure 18 shows a profile of the vertical motion taken from the central

region of the model. For this case the vertical temperature advection

does not dominate the downward diffusion and only a slight packing of

isotherms occurs. A steady state solution, reached after 50 years, is

shown in Figure 19 with a well defined thermocline present. This is

clearly representative of the typical situation below an atmospheric

subtropical high pressure system with near surface temperatures gradual-

ly decreasing eastward from the center of the oceanic anticyclonic gyre.

Without internal heating the effect of a temperature

gradient is as follows. When the east-west surface temperature gradient

is positive, the internal vertical motion becomes negative regardless of

the surface value for w_o. The resulting temperature profiles are similar

to Figure 10. A negative surface gradient produces positive interior

values for w and the baroclinic solutions without internal heating are

similar to Figure 8.

2. Influence of Internal Heating

The influence of heating by mesoscale eddies was tested for the

baroclinic case with a negative horizontal temperature gradient and
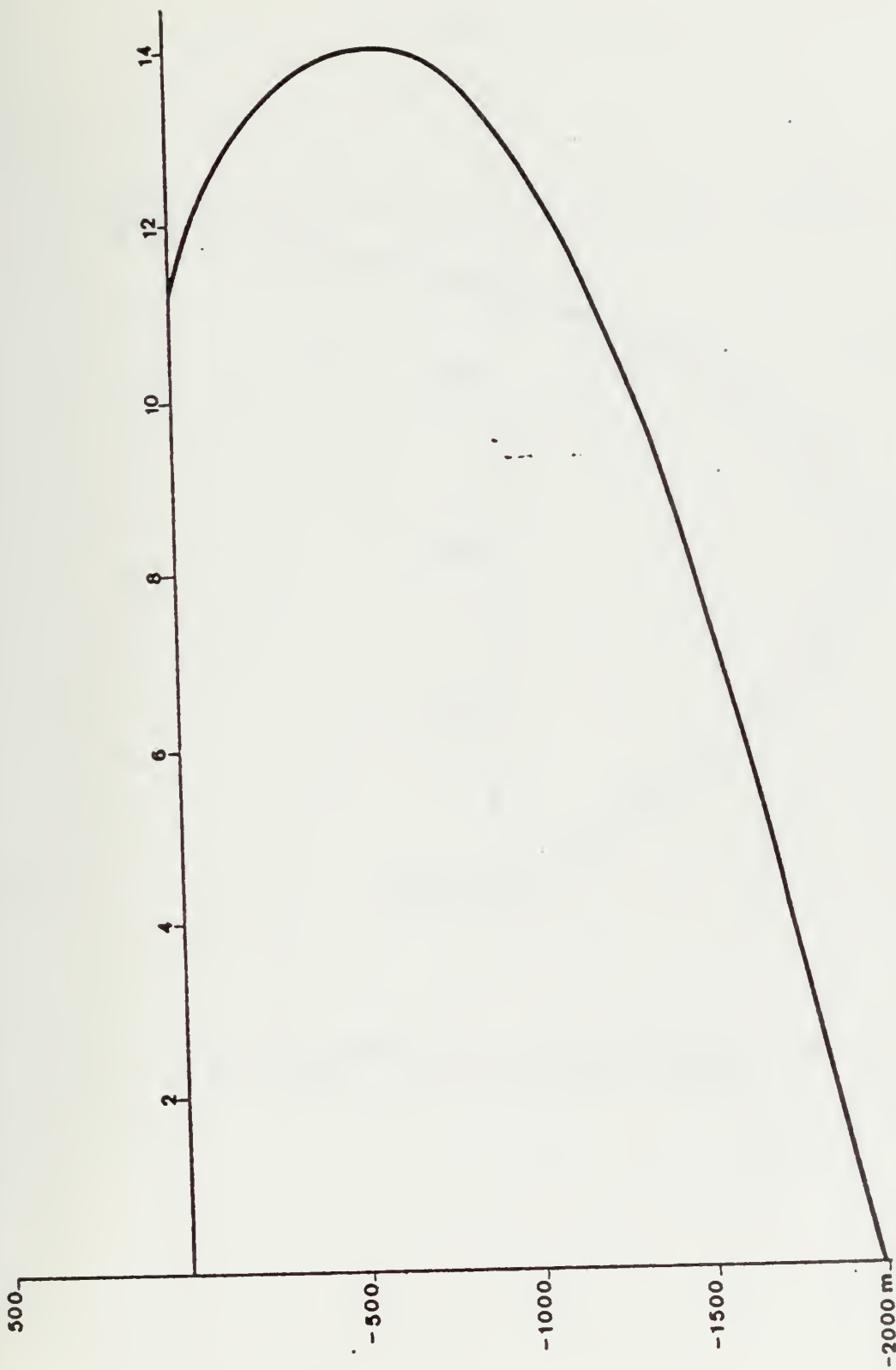
Figure 17. Numerically calculated internal vertical motion in cm sec^{-1} x 10^{-5} for $(\partial T / \partial x)_o < 0$ and $w_o = 10$ cm day^{-1}.
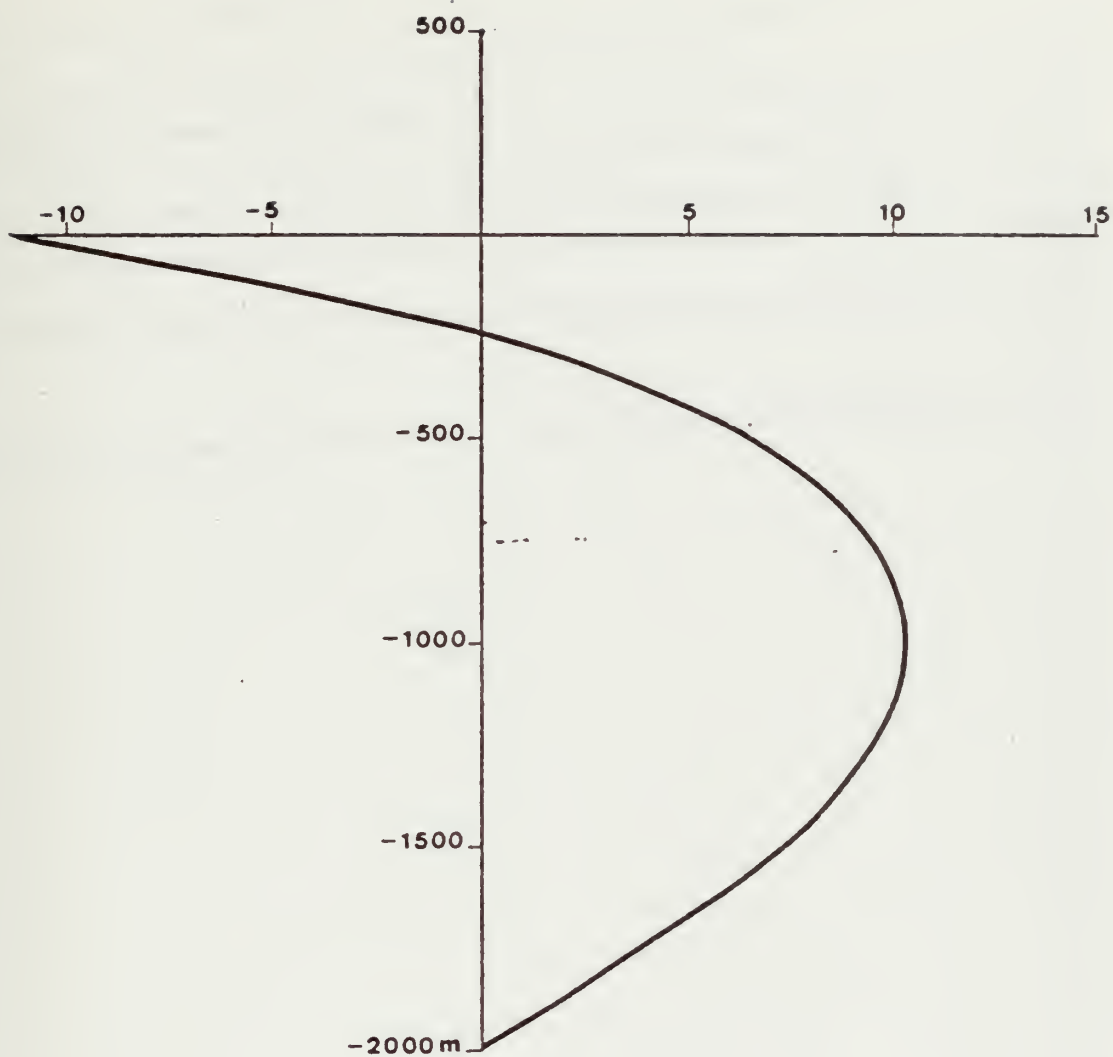
44

Figure 18. Internal vertical motion for $(\partial T/\partial x)_o < 0$ and $w_o =$ −10 cm day^{-1}. w is in cm sec^{-1} x 10^{-5}.
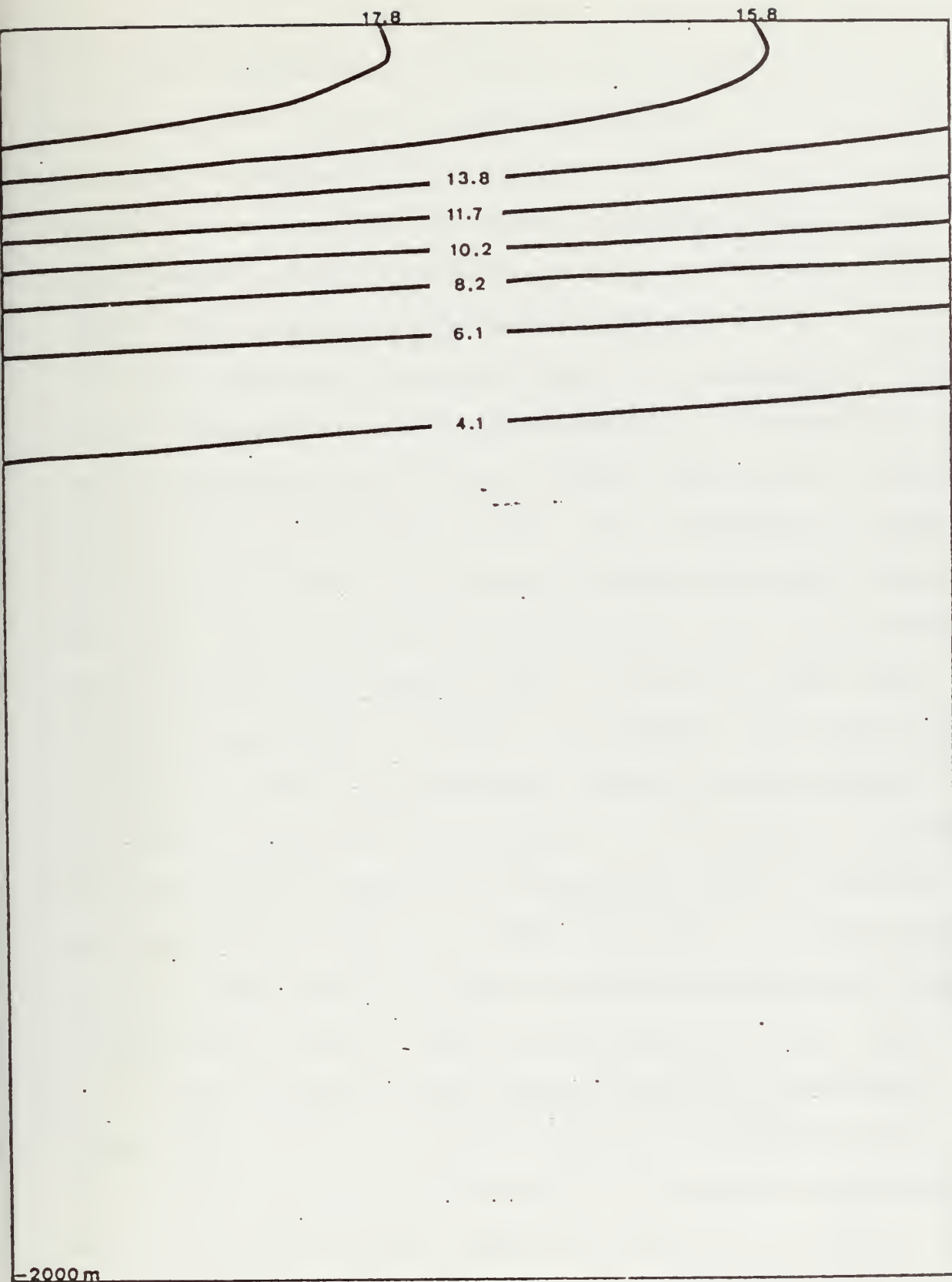
Figure 19. Numerical solution for $(\partial T/\partial x)_o < 0$ and $w_o < 0$.
Temperature is in °C. $(\partial/\partial z) \overline{(w'T')} = 0.$

positive Ekman forcing. Equations (12) and (13) were solved using the initial value approach with the interior vertical motion calculated at each time step as a function of depth and temperature. After 40 years of integration, using a Δt of ten days, the result was a vertical motion profile shown in Figure 20. Recall that in the local solution case which included the eddy term with $w_o > 0$ the interior value of w was simply a linear function of depth (Section III, C).

The accompanying solution for temperature in the baroclinic case is shown in Figure 21. In this case the influence of the eddies was to act in the same sense as the interior vertical motion and cool the near surface layer to an unrealistic -142°C. This is comparable to the local case with $w_o > 0$ (Figure 11), in which the minimum temperature reached was -174°C. It is evident that the baroclinicity acts to moderate the cooling influence of the mesoscale eddies but only to a small extent. Gill et al showed that the amplitude used for $\overline{w'T'}$ in this paper was required in order that in situ baroclinic instability produce eddies of the intensity observed in the open ocean. It is of interest to determine the sensitivity of the solution to the amplitude of $\overline{w'T'}$. Test cases were run in which the amplitude of $\overline{w'T'}$ was varied. It was found that reducing the amplitude by two orders of magnitude was required to produce a mean temperature profile close to that observed in the real ocean.

Cases were also run with internal heating and the following conditions; $\frac{\partial T_o}{\partial x} < 0$ with $w_o < 0$, $\frac{\partial T_o}{\partial x} > 0$ with $w_o > 0$ and $\frac{\partial T_o}{\partial x} > 0$ with $w_o < 0$. In all of these cases the resolution of the model was insufficient to handle the strong vertical temperature gradients which developed near the sea surface. Finer vertical resolution and thus smaller time steps would be required to obtain a numerical solution for any of the above three cases.
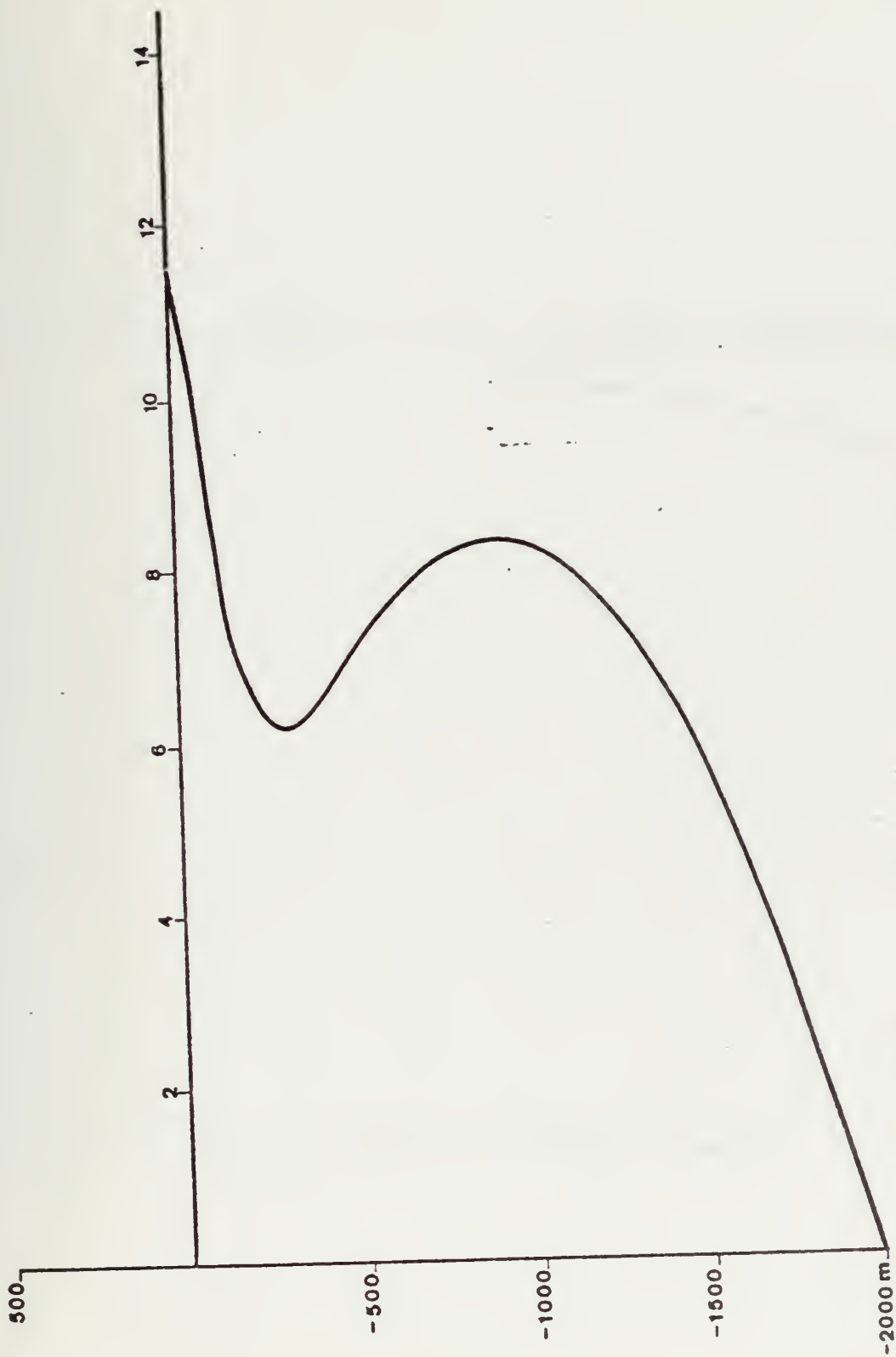
47

Figure 20. Internal vertical motion for $(\partial T/\partial x)_o < 0$ and $w_o > 0$. w is in cm sec^{-1} x 10^{-5}.
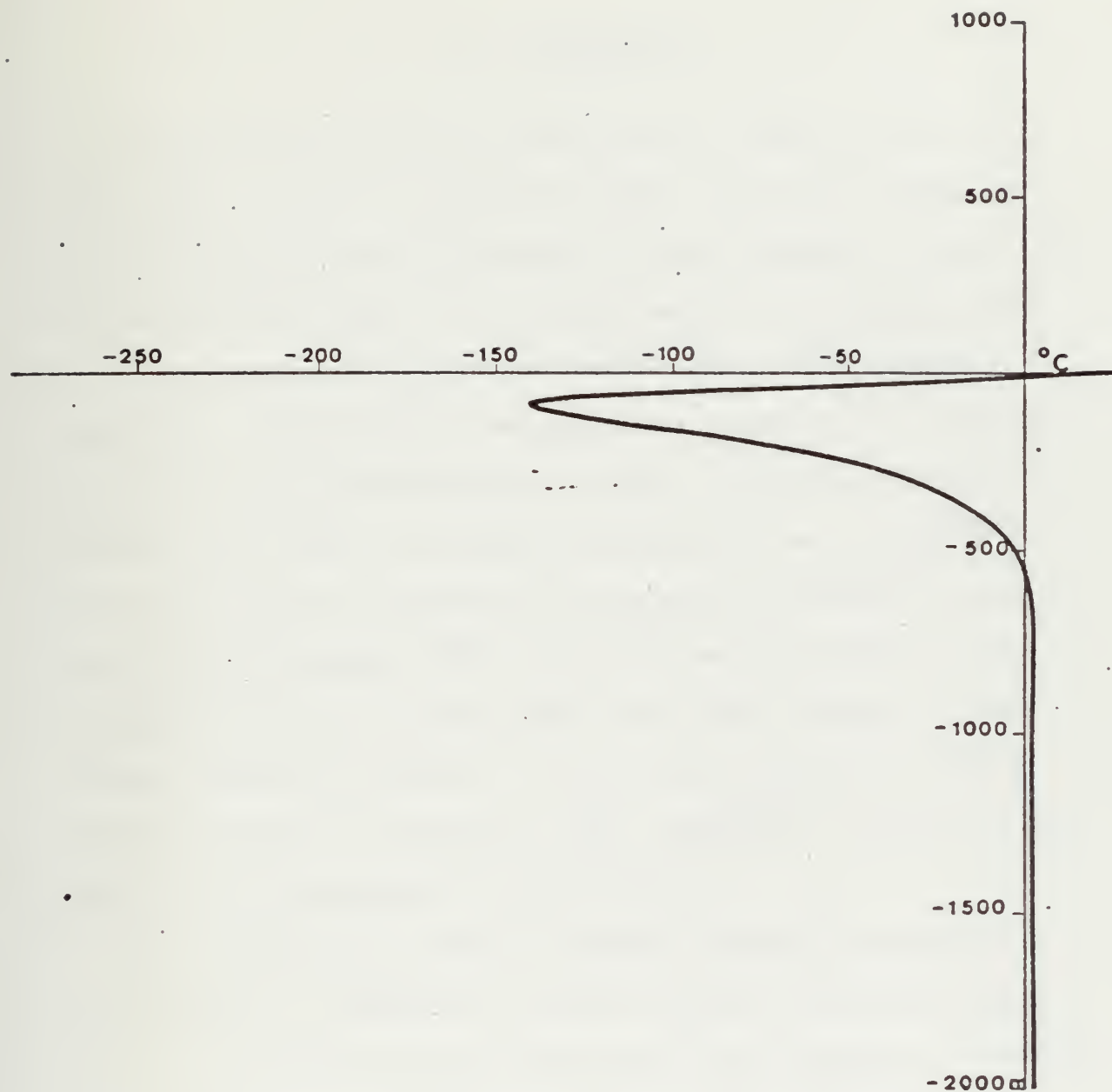
Figure 21. Numerical solution for $(\partial T/\partial x)_o < 0$ and $w_o = 10$ cm day^{-1}.

IV. CONCLUSIONS

It is obvious that the real ocean does not freeze as a result of vertical heat transport by mesoscale eddies. There are a number of possible explanations for the excessive cooling observed in some of the test cases in this study. In deriving a model that was simple enough to test the influence of eddies, it was necessary to make numerous assumptions. With the motion independent of y and with the temperature specified at the top and bottom of the model, the mesoscale eddy heat transport could only be distributed vertically by the term $\frac{\partial}{\partial z}(\overline{w'T'})$. Were there an advective motion in the meridional direction, the north-ward eddy heat transport, $\overline{v'T'}$, could have been distributed by the term $\frac{\partial}{\partial y}(\overline{v'T'})$ such as to produce much less drastic effects and more realistic temperature profiles. It would be of interest to include horizontal temperature advection, $v\frac{\partial T}{\partial y}$, and $\frac{\partial}{\partial y}(\overline{v'T'})$ and then run the model testing the sensitivity of those terms.

Since the mesoscale heating by transient eddies was determined from an analytic consideration of energy transfer rate by Gill et al (1974), it is possible that the amplitude of that transfer was overesti-mated. As stated before, Gill et al are estimating a maximum eddy strength by assuming that all of the mean flow available potential energy is converted into eddy energy. Since the earth's rotation acts as a constraint to energy conversion and since the most favorable condi-tions for eddy growth are found where the isopycnals slope upward towards the equator, i.e., colder water near the equator, a complete

conversion of mean available potential energy to eddy kinetic energy

may not be possible. Using the amplitude for $\overline{w'T'}$ from Gill et al,

the unrealistic results from the model strongly suggest that the eddies

observed in the open ocean are not the result of in situ baroclinic

instability.

The results of this thesis give a preliminary indication of the

potential magnitude of influence that energetic mesoscale eddies have

on the temperature structure of the ocean. It is evident that the

heat equation in the ocean should include mesoscale eddy heating terms

if accurate and complete solutions are to be obtained.

REFERENCES

1. Bernstein, R. L., and W. B. White, 1974: "Time and length scales of baroclinic eddies in the central north Pacific Ocean." J. Phys. Oceanogr., 4, 613-624.

2. Gill, A. E., J. S. A. Green, and A. J. Simmons, 1974: "Energy partician in the large-scale ocean circulation and the production of mid-ocean eddies." Deep-Sea Research, 21, 499-528.

3. Haney, R. L., 1974: "A numerical study of the response of an idealized ocean to large-scale surface heat and momentum flux." J. Phys. Oceanogr., 4, 145-167.

4. Kraus, E. B., and C. Rooth, 1961: "Temperature and steady state vertical heat flux in the ocean surface layers." Tellus, 13, 231-238.

5. Phillips, N. A., 1954: "Energy transformations and meridional circulations associated with simple baroclinic waves in a two-level quasi-geostrophic model." Tellus, 6, 273-286.

6. Robinson, A., and H. Stommel, 1959: "The oceanic thermocline and associated thermohaline circulation." Tellus, 11, 295-308.

7. Stommel, H., and J. Webster, 1962: "Some properties of thermocline equations in a subtropical gyre." J. Marine Research, 20, 42-56.

8. Veronis, G., 1969: "On theoretical models of the thermocline circulation." Deep-Sea Research, 16, 301-323.

9. Woods Hole Notes, 1973: "MODE, MID-OCEAN DYNAMICS EXPERIMENT." 7, 1-6.

INITIAL DISTRIBUTION LIST

No. Copies

1. Defense Documentation Center   2
   Cameron Station
   Alexandria, Virginia 22314

2. Library (Code 0212)   2
   Naval Postgraduate School
   Monterey, California 93940

3. Dr. G. J. Haltiner, Code 51Ha   1
   Department of Meteorology
   Naval Postgraduate School
   Monterey, California 93940

4. Dr. R. L. Haney, Code 51Hy   2
   Department of Meteorology
   Naval Postgraduate School
   Monterey, California 93940

5. Lt. W. E. Christensen USN   1
   Fleet Weather Central
   COMNAVMARIANAS Box 2
   FPO San Francisco 96630

6. Director, Naval Oceanography and Meteorology   1
   Building 200
   Washington Navy Yard
   Washington, D. C. 20374

7. Meteorology Department Code 51 Library   1
   Naval Postgraduate School
   Monterey, California 93940